0.1 Basic formulation for plates and shells

0.1.1 Some assumptions for the kinematic model of the plate

A necessary condition for applying the plate/shell model framework to a deformable body is that a geometrical midsurface might be, if only loosely, recognized for such a body. Then, an iterative refinement procedure[1] may be applied to such tentative midsurface guess.

Then, material should be observed as *[piecewise-]*homogeneous, or slowly varying in mechanical properties while moving at a fixed distance from the midsurface.

Of the two outer surfaces, one has to be defined as the *upper* or *top* surface, whereas the other is named lower ot *bottom*, thus implicitly orienting the midsurface normal towards the top.

Finally, the body should result fully determined based on a) its midsurface, b) its pointwise thickness, and c) the through-thickness (TT) distribution of the constituent materials.

The geometrical midsurface is of little significance if the material distribution is not symmetric[2]; such midsurface, in fact, exhibits no relevant properties in general. Its definition is nevertheless pretty straighforward.

In the present treatise, a more general *reference* surface definition is preferred to its median geometric counterpart; in particular, an *offset* term o is considered that pointwisely shifts the geometric midsurface with respect to the reference surface. A positive offset shifts the midsurface towards the top.

With the introduction of the offset term, the reference surface may be arbitrarily positioned with respect to the body itself; as an example, an offset set equal to plus or minus half the thickness makes the reference surface correspondent to the bottom or top surfaces, respectively.

Such offset term becomes fundamental in the Finite Element (FE) shell implementation, where, in fact, the reference plane is uniquely

[1] Normal segments may be cast from each point along the midsurface, that end on the outer body surfaces. The midpoint locus of these segments redefines the midsurface itself.

[2] If the unsimmetric laminate is composed by isotropic layers, a reference plane may be obtained for which the $\underline{\underline{b}}$ membrane-to-bending coupling matrix vanishes; a similar condition may not be verified in the presence of orthotropic layers.

defined by the position of the nodes, whereas the offset arbitrarily shifts the geometrical midsurface.

In the case of limited[3] curvatures, and for considerations whose scope is local, the tangent reference plane may be employed in place of the possibly curve reference surface, thus locally reducing the general shell treatise to its planar, plate counterpart.

Figure 1 shows the basic kinematic relations for the shear deformable (Mindlin) plate model; in the undeformed configuration, P is a generic material point along the plate thickness, and Q is its normal projection on the reference plane. Such Q point is named *reference point* for the TT normal segment it belongs to.

A local reference system is defined, whose third axis z is normal to the undeformed midsurface; the first in-plane (IP) x axis may be arbitrarily oriented, e.g. by projecting a global $\hat{v}$ unit vector, and the remaining y axis may be construed such that it finalizes the right xyz triad.

Then, the deformed configuration is considered, and the motion of both the points is monitored according to two mutually orthogonal views.

The P displacement components $(u_\mathrm{P}, v_\mathrm{P}, w_\mathrm{P})$ may be defined as a function of the motion of its reference point Q, described in terms of its displacement components (u, v, w), plus the two θ, ϕ rotation components with respect to the x, y IP local axes, respectively. Those angular displacements are defined with respect to the normal segment orientation, as measured on the orthogonally projected views. After some cumbersome trigonometric manipulations[4] we obtain

$$
\begin{aligned}
u_P &= u + z\,(1+\check{\epsilon}_z)\,\frac{\cos\theta}{\sqrt{1-\sin^2\phi\sin^2\theta}}\sin\phi \\
v_P &= v - z\,(1+\check{\epsilon}_z)\,\frac{\cos\phi}{\sqrt{1-\sin^2\phi\sin^2\theta}}\sin\theta \\
w_P &= w + z\left((1+\check{\epsilon}_z)\,\frac{\cos\phi\cos\theta}{\sqrt{1-\sin^2\phi\sin^2\theta}} - 1\right),
\end{aligned}
$$

[3] with respect to thickness

[4] in which it may happen to miss some higher order terms, as the author persistently did in previous versions of the present notes

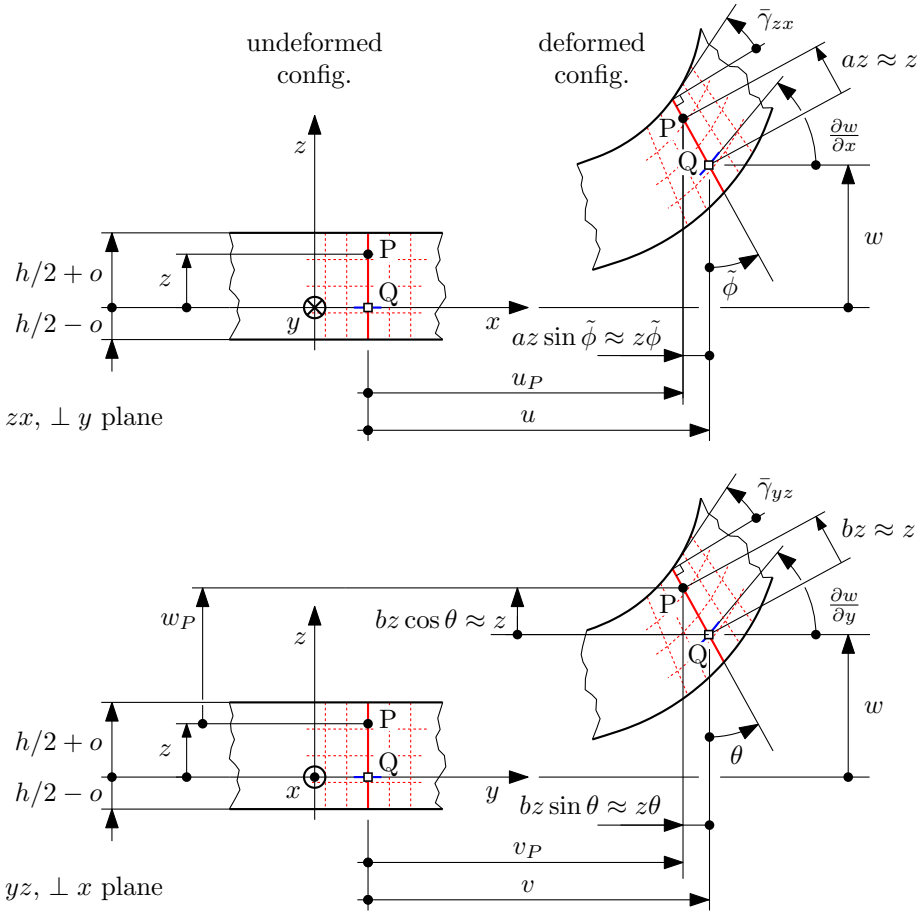

$$\{a, b\} = \frac{(1+\check{\epsilon})}{\sqrt{1-\sin^2\phi\sin^2\theta}}\{\cos\theta, \cos\phi\} \approx 1$$

Figure 1: Relevant dimensions for describing the deformable plate kinematics. Here, two a, b factors are introduced which reduce to unity for small rotations and strain.

where $z\,(1+\check{\epsilon}_z)$ is the length of the PQ segment on the deformed configuration, which is further scaled by the fractional factors due to projection along Fig. 1 views.

The $\check{\epsilon}_z$ average z strain term is defined based on the accumulation of the Poisson shrinkage (or elongation) along the PQ segment, i.e.

$$\begin{aligned}\check{\epsilon}_z(z) &= \frac{1}{z}\int_0^z \epsilon_z d\varsigma \\ &= \frac{1}{z}\int_0^z -\frac{\nu}{1-\nu}\left(\epsilon_x+\epsilon_y\right) d\varsigma,\end{aligned}$$

the second expression holding in the case of isotropic materials only.

The stress component σ_z which is normal to the reference surface is in fact assumed to be either zero or negligible. Being a full discussion[5] of such a plane stress assumption beyond the scope of the present contribution (BSPC), we limit our treatise to the observation that, in the inevitably anecdotal case of Fig. 2, the ratio between the OOP σ_z stress component and its IP counterparts varies with the square of the ratio between the thickness and an in plane significant length. The engineering relevance of such a normal stress component rapidly vanishes with increasing plate thinness. The Fig. 2 examples also points out the intermediate magnitude decay of the OOP shear stresses, whose normalized form linearly varies with the same thinness ratio.

Such displacement components may be linarized with respect to i) the small rotations and ii) small ϵ_z strain hypotheses, thus obtaining the following expressions

$$u_P = u + z\phi \tag{1}$$

$$v_P = v - z\theta \tag{2}$$

$$w_P = w. \tag{3}$$

[5]Such assumption is coherent with the free surface conditions at the top and the bottom skins, and with the moderate thickness of the elastic body, that allows only a narrow deviation from the boundary values. In fact, the equilibrium of a partitioned, TT material segment requires that

$$\sigma_z(z) = -\int_{-h/2+o}^{z} \frac{\partial \tau_{zx}}{\partial x} + \frac{\partial \tau_{yz}}{\partial y} dz = +\int_{z}^{+h/2-o} \frac{\partial \tau_{zx}}{\partial x} + \frac{\partial \tau_{yz}}{\partial y} dz,$$

where τ_{zx}, τ_{yz} are the interlaminar, OOP shear stress components, whose IP gradient is limited.

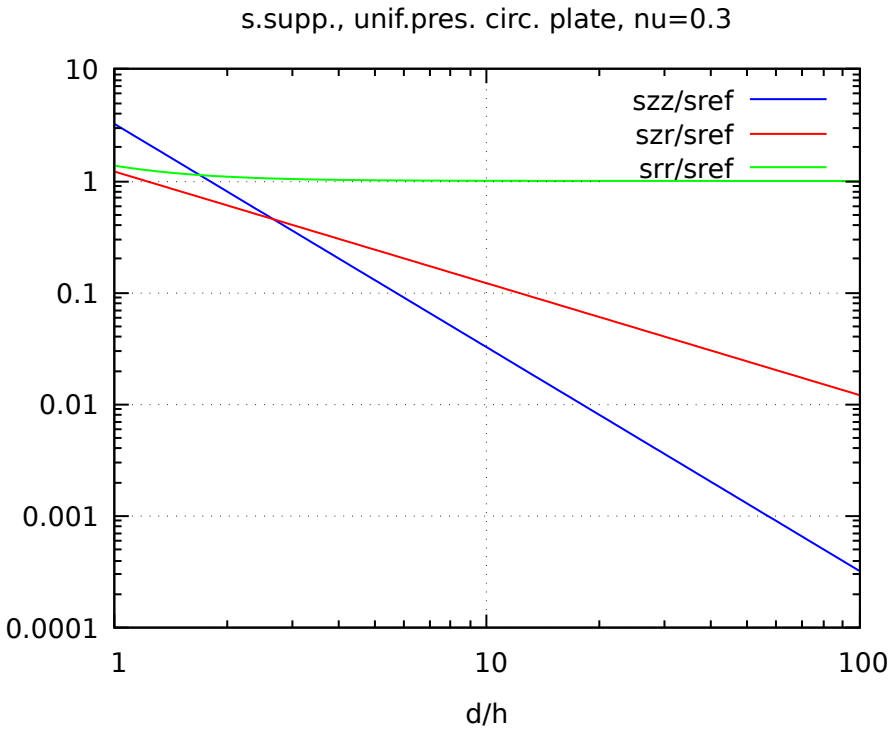

Figure 2: Normalized stress component magnitude in the case of a simply supported circular plate subject to normal pressure, according to the spatial theory of elasticity framework, see [1, p.349]. A homogeneous and isotropically elastic circular plate of diameter d and thickness h is simply supported along its perimeter (i.e. apart from the their transverse component, displacements are free, and so are rotations), and it is loaded by a unit pressure at its upper surface. The peak magnitude of the transverse stress σ_{z} is observed at the pressurized surface, and it equates the pressure value. The OOP shear stress τ_{zr} is maximal along the perimeter, and it equates $\frac{3}{8}\left(\frac{d}{h}\right)$. The two equal IP direct stress components $\sigma_{\mathrm{r}} = \sigma_{\theta}$ reach the peak value of $\frac{3(\nu+3)}{32}\left(\frac{d}{h}\right)^2 + \frac{\nu+2}{20}$ in correspondence of the plate center, at the surface; its thin plate counterpart, σ_{ref}, which lacks the second term, is taken as the normalizing stress value. The remaining $\tau_{\mathrm{r}\theta}$, $\tau_{\theta\mathrm{z}}$ stress components are zero due to axisymmetry. The commonwise $\nu = 0.3$ Poisson ratio value is used in tracing the Figure.

A treatise of the large rotation and/or large strain nonlinear case is, again, BSPC.

According to such linearized expression, the kinematics of the P points originally[6] laying on a TT segment that is normal at Q to the reference surface may be described as that of a rigid body.

The intrinsic shear related warping is either negated or neglected, along with any sliding motion of the P points along the segment[7].

Also, the behaviour of such a segment is coherent with its rigid body modeling from the external loads point of view; in particular the external actions act on the plate deformable body only through their TT resultants, and no stress/strain components, or work, are associated by the shell framework to wall squeezing actions, e.g. laminations.

We thus observe that, according to the shell framework, the following external actions are not distinguishable: i) a q pressure applied at the upper surface, ii) a $-q$ traction applied at the lower surface, iii) a q differential pressure between the outer surfaces, with $p+q$ applied at the top, and a generic p applied at the bottom, and iv) a transverse inertial force whose area density is q, namely due to a oppositely oriented $\frac{q}{\rho h}$ acceleration, where ρ is the material density. Also, a fp, friction induced, x-oriented shear action at the upper surface is not distinguishable from an analogous distributed force for unit area applied at the reference surface, plus a y-oriented distributed moment per unit area, whose magnitude is $fp(h/2+o)$.

By observing the deformed configurations in Fig. 1, the normal displacement $\left(\frac{\partial w}{\partial x}, \frac{\partial w}{\partial y}\right)$ gradient – i.e. the gained slope of the deformed reference surface, with respect to its original orientation – is made up of two terms, namely the rotation of the normal segment, which originates from the accumulation of the flexural curvature, and the shear compliance, which resembles the transverse slippage typical of a card deck. The following expressions are derived

[6] i.e. in the undeformed configuration

[7] The elision of higher order terms renders the laminate kinematically – but not elastically – indistinguishable from its counterpart that might derive from a plane *strain* assumption.

$$\frac{\partial w}{\partial x} = \bar{\gamma}_{zx} - \phi \tag{4}$$

$$\frac{\partial w}{\partial y} = \bar{\gamma}_{yz} + \theta \tag{5}$$

in which the bar notation employed for the OOP shear components emphasizes their TT average nature.

0.1.2 Local and generalized strains

The IP strain components may hence be derived at the P point through differentiation, and in particular we have

$$\epsilon_x = \frac{\partial u_P}{\partial x} = \frac{\partial u}{\partial x} + z\frac{\partial \phi}{\partial x} \tag{6}$$

$$\epsilon_y = \frac{\partial v_P}{\partial y} = \frac{\partial v}{\partial y} - z\frac{\partial \theta}{\partial y} \tag{7}$$

$$\gamma_{xy} = \frac{\partial u_P}{\partial y} + \frac{\partial v_P}{\partial x} \tag{8}$$

$$= \left(\frac{\partial u}{\partial y} + \frac{\partial v}{\partial x}\right) + z\left(+\frac{\partial \phi}{\partial y} - \frac{\partial \theta}{\partial x}\right) \tag{9}$$

It clearly appears from the expressions above that the pointwise strain values are due to the sum of i) the strain components as observed at the reference plane,

$$\underline{\mathrm{e}} = \begin{bmatrix} \frac{\partial u}{\partial x} \\ \frac{\partial v}{\partial y} \\ \frac{\partial u}{\partial y} + \frac{\partial v}{\partial x} \end{bmatrix} = \begin{bmatrix} e_x \\ e_y \\ g_{xy} \end{bmatrix} \equiv \underline{\epsilon}_{\mathrm{Q}} \tag{10}$$

which are named *membrane* strains[8] in the customary case in which the material is symmetric[9] with respect to the reference plane, plus ii)

[8] $\underline{\mathrm{e}}$ is an alternative symbol for the more natural, and previously employed $\underline{\bar{\epsilon}}$, whose double barred appearance is however terrible. To complete the transition, also the $\bar{\epsilon}_x$, $\bar{\epsilon}_y$ and $\bar{\gamma}_{xy}$ symbols have been changed onto their e_x, e_y, g_{xy} counterpart.

[9] or, more generally, elastically balanced

terms that linearly scale with the z distance from such a plane, whose coefficients

$$\underline{\kappa} = \begin{bmatrix} +\frac{\partial \phi}{\partial x} \\ -\frac{\partial \theta}{\partial y} \\ +\frac{\partial \phi}{\partial y} - \frac{\partial \theta}{\partial x} \end{bmatrix} = \begin{bmatrix} \kappa_x \\ \kappa_y \\ \kappa_{xy} \end{bmatrix} \tag{11}$$

are named *curvatures*.[10] The strains at the reference surface, and the curvatures constitute the set of plate [shell] *generalized strain components*, which are e.g. usually returned by Finite Element (FE) solvers; those components allow for the following compact representation of the IP strains at P

$$\underline{\epsilon}_{\mathrm{P}} \equiv \underline{\epsilon} = \underline{\mathrm{e}} + z\,\underline{\kappa}\,. \tag{12}$$

It worth to be stressed that the kinematic assumptions for the plate model impose a linear TT profile for each single IP strain component; those components may hence be sampled at the outer surfaces alone, without loss of information. It is here anticipated that an analogous behaviour is proper of the IP stress components if and only if (IIF) the material is elastically homogeneous along the thickness .

The two κ_x and κ_y curvatures equate to the inverse of the normal curvature radii, as probed along the respective local directions; those curvatures are positive if the upper plate fibers are stretched, or, equivalently, if the reference surface acquires convexity if observed from above – i.e. from a point on the positive z axis.

Figure 3 clarifies the nature of the *mixed* curvature term κ_{xy}, which is e.g. typical of open thin walled members – and flat plates as a particular case – subject to torsion[11].

[10] Please note that in the case of shells, the bare *curvature* name may be confusing, since it might refer to either

- the initial, original, geometric, undeformed curvature, which is proper of the shell before the application of some external loads, or to the
- strain, strain-induced, elastic[-plastic], bending, flexural curvature, or curvature change, which consist in the variation of the thin wall curvature due to the effect of the applied loads.

Except for [locally] flat panels, the author suggests to always specify which kind of curvature we refer to. Here, *curvature* is used with reference to *curvature change*.

[11] the *torsional* curvature denomination for the κ_{xy} term, that the present author has widely employed in the past, is not so proper nor widespread, so it might be better avoided. Flexure and torsion are in fact not as uncoupled in the plate realm

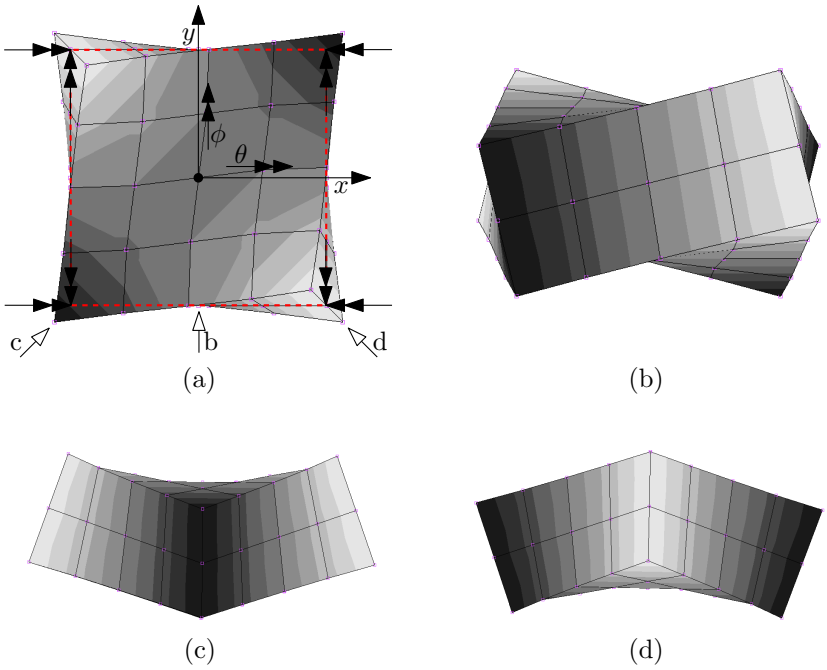

Figure 3: Positive κ_{xy} mixed curvature for the plate element. The grayscale coloring is proportional to the normal displacement w, which spans from an extremal downward deflection (black), to an equal in modulus extremal upward deflection (white). The gray level at the centroid is associated to zero. Subfigure (a) shows the positive γ_{xy} shear strain at the upper surface, the IP undeformed midsurface, and the negative γ_{xy} at the lower surface; the point of sight related to subfigures (b) to (d) are also evidenced. θ and ϕ rotation components decrease with x and increase with y, respectively, thus leading to positive κ_{xy} contributions. As shown in subfigures (c) and (d), the mixed curvature of subfigure (b) evolves into two anticlastic bending curvatures if the reference system is aligned with the square plate element diagonals, and hence rotated by 45° with respect to z.

0.1.3 Stresses, and their through-thickness resultants

The IP stress components at P are derived from strains by referring to the material elastic constants, and to the plane stress hypothesis. We hence have

$$\left[\begin{array}{c} \sigma_x \\ \sigma_y \\ \tau_{xy} \end{array} \right] = \underline{\sigma} = \underline{\underline{\mathrm{D}}}\, \underline{\epsilon} = \underline{\underline{\mathrm{D}}}\, \underline{\mathrm{e}} + z\, \underline{\underline{\mathrm{D}}}\, \underline{\kappa}\,, \tag{13}$$

where $\underline{\underline{\mathrm{D}}}$ embodies the material constitutive law which elastically relates to IP stress/strain components, and which is derived according to the plane stress hypothesis.

In the particular case of an isotropic material – the generally orthotropic case is treated below – such a matrix takes the form

$$\underline{\underline{\mathrm{D}}} = \frac{E}{1-\nu^2} \left[\begin{array}{ccc} 1 & \nu & 0 \\ \nu & 1 & 0 \\ 0 & 0 & \frac{1-\nu}{2} \end{array} \right], \tag{14}$$

whereas the normal component of strain, which is due to the Poisson shrinkage alone, may be evaluated as

$$\epsilon_z = -\frac{\nu}{1-\nu} \left(\epsilon_x + \epsilon_y \right). \tag{15}$$

The attentive reader may observe that no mention is made to the OOP shear stresses, to which a paragraph is devoted below.

Moreover, the absence of transverse shear terms in current paragraph formulation, and in particular in Eq. 13, hints for the IP and the OOP stress/strain components to be elastically uncoupled; the material has evidently been *implicitly* assumed as monoclinic with respect to the reference surface. Such a condition holds e.g. for isotropic materials, and for the orthotropic plies usually employed in laminates.

As in the classical theory of beams, stress components are integrated along the relevant unit of analysis, namely the cross section there, and the normal segment here, to obtain suitable internal action resultants.

---

as they are in beam theory, and *flexure* might be conveniently employed as an umbrella term that also encompass profile (open and thin) wall deformation due to pure torsion.

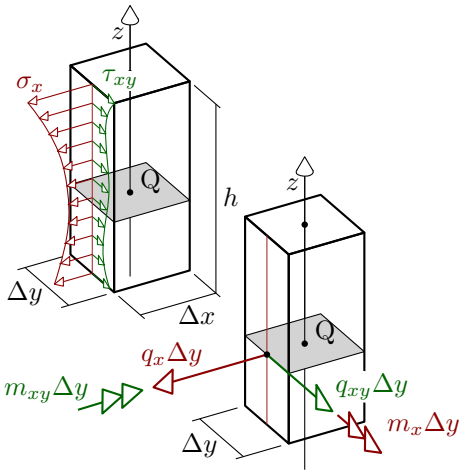

Figure 4: XXX

According to the thin plate framework, stress resultants take the form of forces per unit length along the surface, and they may be expressed as

$$\begin{aligned} \underline{\mathrm{q}} = \begin{bmatrix} q_x \\ q_y \\ q_{xy} \end{bmatrix} &= \int_h \underline{\sigma}\, dz \\ &= \underbrace{\int_h \underline{\underline{\mathrm{D}}}\, dz}_{\underline{\underline{\mathrm{a}}}}\, \underline{\mathrm{e}} + \underbrace{\int_h \underline{\underline{\mathrm{D}}}\, z dz}_{\underline{\underline{\mathrm{b}}}}\, \underline{\kappa} \end{aligned} \tag{16}$$

in the case of the IP components, whereas for the OOP components we have

$$\underline{\mathrm{q}}_z = \begin{bmatrix} q_{xz} \\ q_{yz} \end{bmatrix} \qquad q_{xz} = \int_h \tau_{zx} dz \qquad q_{yz} = \int_h \tau_{yz} dz. \tag{17}$$

Those quantities may be interpreted with respect to their (doubled if single) subscripts as follows: q_{ab} is the b component of internal action that is transmitted through a TT imaginary gate, whose in plane width is unit and whose normal is oriented along a. According to this rationalization, the $\underline{\mathrm{q}}$ components are also called *stress flows*.

Besides the internal action resultants of the force kind, by weighting the stress component contribution based on their z lever arm we obtain

the moment stress resultants (or *moment flows*), whose expressions follow

$$\underline{\mathrm{m}} = \begin{bmatrix} m_x \\ m_y \\ m_{xy} \end{bmatrix} = \int_h \underline{\sigma}\, z dz$$
$$= \underbrace{\int_h \underline{\underline{\mathrm{D}}}\, z dz}_{\underline{\underline{\mathrm{b}}} \equiv \underline{\underline{\mathrm{b}}}^{\mathrm{T}}} \underline{\mathrm{e}} + \underbrace{\int_h \underline{\underline{\mathrm{D}}}\, z^2 dz}_{\underline{\underline{\mathrm{c}}}} \underline{\kappa}\,. \tag{18}$$

A selection of internal action components is represented in Fig. 4 shows, along with the stress distributions they arise from.

0.1.4 Constitutive equations for the plate

By employing the matrices defined in Eqs. 16 and 18, the cumulative generalized strain - stress resultants relations for the plate (or for the laminate) may be summarized in the following expressions

$$\begin{bmatrix} \underline{\mathrm{q}} \\ \underline{\mathrm{m}} \end{bmatrix} = \begin{bmatrix} \underline{\underline{\mathrm{a}}} & \underline{\underline{\mathrm{b}}} \\ \underline{\underline{\mathrm{b}}}^{\mathrm{T}} & \underline{\underline{\mathrm{c}}} \end{bmatrix} \begin{bmatrix} \underline{\mathrm{e}} \\ \underline{\kappa} \end{bmatrix} \tag{19}$$

which are usually referred to as the *constitutive equations* of the [laminate] plate, and the coefficient matrix, named *constitutive matrix* for the laminate, summarizes the elastic response of the latter.

The contribution of the IP stress/strain components to the elastic strain energy area density[12] is defined based on the previous relation as

$$v^{\dagger} = \frac{1}{2} \begin{bmatrix} \underline{\mathrm{q}} \\ \underline{\mathrm{m}} \end{bmatrix}^{\top} \begin{bmatrix} \underline{\mathrm{e}} \\ \underline{\kappa} \end{bmatrix} \tag{20}$$
$$= \frac{1}{2} \begin{bmatrix} \underline{\mathrm{e}} \\ \underline{\kappa} \end{bmatrix}^{\top} \begin{bmatrix} \underline{\underline{\mathrm{a}}} & \underline{\underline{\mathrm{b}}} \\ \underline{\underline{\mathrm{b}}}^{\mathrm{T}} & \underline{\underline{\mathrm{c}}} \end{bmatrix} \begin{bmatrix} \underline{\mathrm{e}} \\ \underline{\kappa} \end{bmatrix}. \tag{21}$$

The $\underline{\underline{\mathrm{a}}}$ and the $\underline{\underline{\mathrm{c}}}$ minors of the constitutive matrix characterize the plate stiffness with respect to membrane and flexural load case families respectively; the membrane/flexural coupling stiffness minor

[12] i.e. strain energy per unit reference surface area

$\underline{\underline{\mathrm{b}}}$, which is in general nonzero, vanishes if the material is symmetrically distributed with respect to the reference surface.

In the commonwise case of TT homogeneous material, and null offset[13] we have

$$\underline{\underline{\mathrm{a}}} = h\,\underline{\underline{\mathrm{D}}} \qquad \underline{\underline{\mathrm{b}}} = \underline{\underline{0}} \qquad \underline{\underline{\mathrm{c}}} = \frac{h^3}{12}\,\underline{\underline{\mathrm{D}}},$$

i.e. the membrane stiffness varies linearly with the wall thickness, the flexural stiffness varies with the cube of the thickness, and the membrane and the flexural loadings are mutually uncoupled. Such a laminate elastic properties dependence on thickness essentially holds also for laminates, if the TT distribution of the various materials is kept comparable.

0.1.5 The transverse shear stress/strain components

A full treatise on the title topic is, due to its complexity, BSPC; starting points for further investigation my be found in [2], [3] or in the theory manual of your favourite FE solver[14].

The two transverse shear components

$$\underline{\gamma}_z = \begin{bmatrix} \bar{\gamma}_{yz} \\ \bar{\gamma}_{zx} \end{bmatrix}$$

are in fact more directly recognizable as further contributions to the $\left(\frac{\partial w}{\partial x}, \frac{\partial w}{\partial y}\right)$ normal deflection gradient, with respect to what is attributable to flexure alone, than TT averages of actual, pointwise shear strains – see e.g. Figure 1. Also, the two

$$\underline{\mathrm{q}}_z = \begin{bmatrix} q_{xz} \\ q_{yz} \end{bmatrix}$$

stress flow components defined in Eq. 17 are recognized to perform work[15] on the same $\bar{\gamma}_{yz}$ and $\bar{\gamma}_{zx}$ transverse shear components, respectively; the transverse shear contribution to the elastic strain energy per

[13] In the presence of a nonzero offset between the reference and the median planes, the uncoupled nature of the plate membrane/flexural loadings is only *formally* lost. If the same problem is considered based on a median reference plane, in fact, such a property is obviously restored.

[14] See e.g. MSC.Marc 2013.1 Documentation, Vol. A, pp. 433-436

[15] in particular, work for unit reference surface area

unit ref. surface area is hence

$$v^{\ddagger} = \frac{1}{2}\,\underline{\mathrm{q}}_z^{\top}\,\underline{\gamma}_z = \frac{1}{2}q_{xz}\bar{\gamma}_{xz} + \frac{1}{2}q_{yz}\bar{\gamma}_{yz}. \tag{22}$$

The constitutive equation for the transverse shear is set at normal segment (vs. punctual) level, with the declared aim of collecting the elastic strain energy contributions along the thickness, and they are usually formulated as

$$v^{\ddagger} = \frac{1}{2}\,\underline{\gamma}_z^{\top}\,\underbrace{\chi\int_h \underline{\underline{\mathrm{G}}}\,dz}_{\underline{\underline{\Gamma}}}\,\underline{\gamma}_z \tag{23}$$

where $\underline{\underline{\mathrm{G}}}$ is the pointwise constitutive matrix for the transverse shear components[16] – which is considered through its TT integral, χ is a *shear correction factor* – which accommodates for possibly any incongruence in the formulation, and $\underline{\underline{\Gamma}}$ is an emended transverse shear constitutive matrix for the whole plate. By comparing Eqns. 22 and 23 we also derive the *de facto* transverse shear constitutive relation

$$\underline{\mathrm{q}}_z = \underline{\underline{\Gamma}}\,\underline{\gamma}_z. \tag{24}$$

for the Mindlin shear deformable plate.

In the case of isotropic materials, $\underline{\underline{\mathrm{G}}}$ is a diagonal matrix whose terms equate the shear modulus, i.e.

$$\underline{\underline{\mathrm{G}}} = \frac{E}{2\,(1+\nu)}\begin{bmatrix} 1 & 0 \\ 0 & 1 \end{bmatrix},$$

whereas the χ shear correction factor is usually assumed as $\frac{5}{6}$ if the material is TT uniform[17]; different χ values are however proposed in literature, see e.g. [4], along with different procedures[18] for evaluating $\underline{\underline{\Gamma}}$.

[16] $\underline{\underline{\mathrm{G}}}$ is the 2 by 2 matrix s.t. $\begin{bmatrix} \tau_{zx} \\ \tau_{yz} \end{bmatrix} = \underline{\underline{\mathrm{G}}}\begin{bmatrix} \gamma_{zx} \\ \gamma_{yz} \end{bmatrix}$.

[17] please note the parallel with the inverse 1.2 correction factor for the shear contribution to the beam elastic strain energy, proper of the solid rectangular cross section.

[18] we report as an example the notable case of of honeycomb panels – whose transverse shear compliance is rarely negligible, in which Γ is defined as the $\underline{\underline{\mathrm{G}}}_{\mathrm{foam}}$ transverse shear constitutive matrix for the foam/honeycomb material interposed between the outer skins, multiplied by the overall panel thickness h; in this case the χ transverse shear correction factor is implicitly defined as unity.

In the case pointwise values are requested for the τ_{zx} and τ_{yz} stress components – e.g. in the analysis of interlaminar stresses in composite laminates, those quantities are derived from the assumed absence of shear stresses on the lower surface, and by accumulating the IP stress component contributions to the x and y translational equilibria up to the desired z sampling height. We hence obtain

$$\tau_{zx}(z) = -\int_{-\frac{h}{2}+o}^{z} \frac{\partial \sigma_x}{\partial x} + \frac{\partial \tau_{xy}}{\partial y} dz \tag{25}$$

$$\tau_{yz}(z) = -\int_{-\frac{h}{2}+o}^{z} \frac{\partial \tau_{xy}}{\partial x} + \frac{\partial \sigma_y}{\partial y} dz. \tag{26}$$

The parallel is evident with the Jourawsky theory of shear for beams.

0.1.6 Hooke's law for the orthotropic lamina

Hooke's law for the orthotropic material IP stress conditions, with respect to principal axes of orthotropy;

$$\underline{\underline{\mathrm{D}}}_{123} = \begin{bmatrix} \frac{E_1}{1-\nu_{12}\nu_{21}} & \frac{\nu_{21}E_1}{1-\nu_{12}\nu_{21}} & 0 \\ \frac{\nu_{12}E_2}{1-\nu_{12}\nu_{21}} & \frac{E_2}{1-\nu_{12}\nu_{21}} & 0 \\ 0 & 0 & G_{12} \end{bmatrix} \tag{27}$$

$$\begin{bmatrix} \sigma_1 \\ \sigma_2 \\ \tau_{12} \end{bmatrix} = \underline{\underline{\mathrm{T}}}_1 \begin{bmatrix} \sigma_x \\ \sigma_y \\ \tau_{xy} \end{bmatrix} \qquad \begin{bmatrix} \epsilon_1 \\ \epsilon_2 \\ \gamma_{12} \end{bmatrix} = \underline{\underline{\mathrm{T}}}_2 \begin{bmatrix} \epsilon_x \\ \epsilon_y \\ \gamma_{xy} \end{bmatrix} \tag{28}$$

where

$$\underline{\underline{\mathrm{T}}}_1 = \begin{bmatrix} m^2 & n^2 & 2mn \\ n^2 & m^2 & -2mn \\ -mn & mn & m^2 - n^2 \end{bmatrix} \tag{29}$$

$$\underline{\underline{\mathrm{T}}}_2 = \begin{bmatrix} m^2 & n^2 & mn \\ n^2 & m^2 & -mn \\ -2mn & 2mn & m^2 - n^2 \end{bmatrix} \tag{30}$$

α is the angle between 1 and x;

$$m = \cos(\alpha) \qquad\qquad n = \sin(\alpha) \tag{31}$$

The inverse transformations may be obtained based on the relations

$$\underline{\underline{\mathrm{T}}}_1^{-1}(+\alpha) = \underline{\underline{\mathrm{T}}}_1(-\alpha) \qquad \underline{\underline{\mathrm{T}}}_2^{-1}(+\alpha) = \underline{\underline{\mathrm{T}}}_2(-\alpha) \tag{32}$$

Finally

$$\underline{\sigma} = \underline{\underline{\mathrm{D}}}\,\underline{\epsilon} \qquad \underline{\underline{\mathrm{D}}} \equiv \underline{\underline{\mathrm{D}}}_{xyz} = \underline{\underline{\mathrm{T}}}_1^{-1}\,\underline{\underline{\mathrm{D}}}_{123}\,\underline{\underline{\mathrm{T}}}_2 \tag{33}$$

With regard to the transverse shear constitutive relation, in the case of an orthotropic material whose OOP shear moduli are G_{z1} and G_{2z} we have

$$\underline{\underline{\mathrm{G}}} = \begin{bmatrix} n^2G_{z1} + m^2G_{2z} & mnG_{z1} - mnG_{2z} \\ mnG_{z1} - mnG_{2z} & m^2G_{z1} + n^2G_{2z} \end{bmatrix}.$$

0.1.7 An application: the four point bending test specimen.

The case of the four point bending test is considered, see Figure 5a, with an isotropic and homogeneous specimen material. Specimen dimensions are defined as in Figure, where the b the specimen width is taken as the relevant unit of length.

The width to length ratio of the specimen is less than unity, but far from being negligible; a treatise according to the plate theory would hence be more appropriate than the beam model which is usually proposed by normative.

Such a test is based on the assumption that the bending moment – a beam framework quantity – is constant along the gauge length, and equal to Fl; such a quantity equates the through-width (TW) integral of the m_{x} moment resultant, whose value is assumed TW constant and equal to $m_{\mathrm{x}}^* = Fl/b$. The specimen curvature along the gauge length is

$$k_{\mathrm{x}}^* = \frac{12Fl}{Ebh^3} \tag{34}$$

according to the beam theory; such a value taken as a reference.

The treatise according to the plate theory is far less straightforward that its trivial beam counterpart, since e.g. we may consider the two opposite extremal cases of i) unconstrained anticlastic secondary curvature, or, equivalently, null m_{y} transverse (in the sense of TW, not TT) moment resultant, and ii) cylindrical bending, i.e. null

transverse κ_{y} curvature. The membrane generalized stress/strain components are zero, as the transverse shear terms along the gauge length. The mixed moment resultant and curvature are zero in both the cases, since they are null at the xz symmetry plane, and they are assumed TW constant. By applying the constitutive relations proper of the homogeneous, isotropic plates, we derive for the unconstrained anticlastic curvature case i)

$$m_{\mathrm{x}} = m_{\mathrm{x}}^{*} \qquad m_{\mathrm{y}} = 0 \qquad \kappa_{\mathrm{x}} = k_{\mathrm{x}}^{*} \qquad \kappa_{\mathrm{y}} = -\nu k_{\mathrm{x}}^{*},$$

whereas for the cylindrical bending case ii) we have

$$m_{\mathrm{x}} = m_{\mathrm{x}}^{*} \qquad m_{\mathrm{y}} = \nu m_{\mathrm{x}}^{*} \qquad \kappa_{\mathrm{x}} = \left(1-\nu^{2}\right) k_{\mathrm{x}}^{*} \qquad \kappa_{\mathrm{y}} = 0.$$

We then observe that the nonzero κ_{y} transverse curvature predicted by i) is inconsistent with the hypothesis of a full width line contact at the supports, whose cylindrical surface is transversely flat; the unconstrained anticlastic curvature confines the specimen contact interaction with the inner supports to a point in correspondence of the width midspan, whereas the outer supports touch the specimen at its edges only. Such a TW inhomogeneous loading condition induces contact actions which may effectively oppose the anticlastic curvature, which locally appears not "unconstrained" anymore.

On the other hand, a m_{y} moment resultant which is predicted according to cylindrical bending not to vanish at the specimen flanks is incompatible with the free surface boundary condition; continuity conditions requires in fact that a distributed moment external action is applied at the specimen flanks, which apparently is not the case.

The actual response of the specimen in terms of moment resultants and curvatures, as probed at its centroidal axis, is plotted in Fig. 5b in the case of bilateral support condition, i.e. $w = 0$ and $w = d$ at the outer and inner indenters, respectively, being d displacement of the inner, moving, support. The cylindrical bending solution ii) is observed at the supports, whereas a progressive transition to the unconstrained anticlastic curvature solution i) is observed while moving away from those supported areas. In particular, the central portion of the gauge length behaves consistently with i).

In Fig. 5c, the same quantities are reported in the actual case

of unilateral contact at supports, i.e. the Signorini conditions[19] are imposed which consist in

$$g(y) \geq 0 \tag{35}$$
$$f(y) \geq 0 \tag{36}$$
$$g(y) \cdot f(y) = 0, \tag{37}$$

where $f(y)$ is the lineic contact force along the width, positive if compressive, and $g(y)$ is the gap between specimen and indenter, namely $g(y) = -w(y)$ and $g(y) = w(y) - d$ at the outer and inner supports, respectively.

According to this second model, supports are less effective in locally imposing a null secondary curvature, thus extending the validity of the unconstrained anticlastic curvature solution i) to most of the gauge length.

0.1.8 Final Notes.

A few sparse notes:

- If the unsymmetric laminate is composed by isotropic layers, a reference plane may be obtained for which the $\underline{\underline{b}}$ membrane-to-bending coupling matrix vanishes; a similar condition may not be verified in the presence of orthotropic layers.
- Thermally induced distortion is not self-compensated in an unsymmetric laminate even if the temperature is held constant through the thickness. Such fact, united to the unavoidable thermal cycles that occurs in manufacturing if not in operation, makes such configurations pretty undesirable.

[19] Those conditions consist in turn in a no compenetration inequality 35, in a no tractive contact action inequality 36, and in the mutual local exclusion of nozero gap and nonzero contact force, 37.

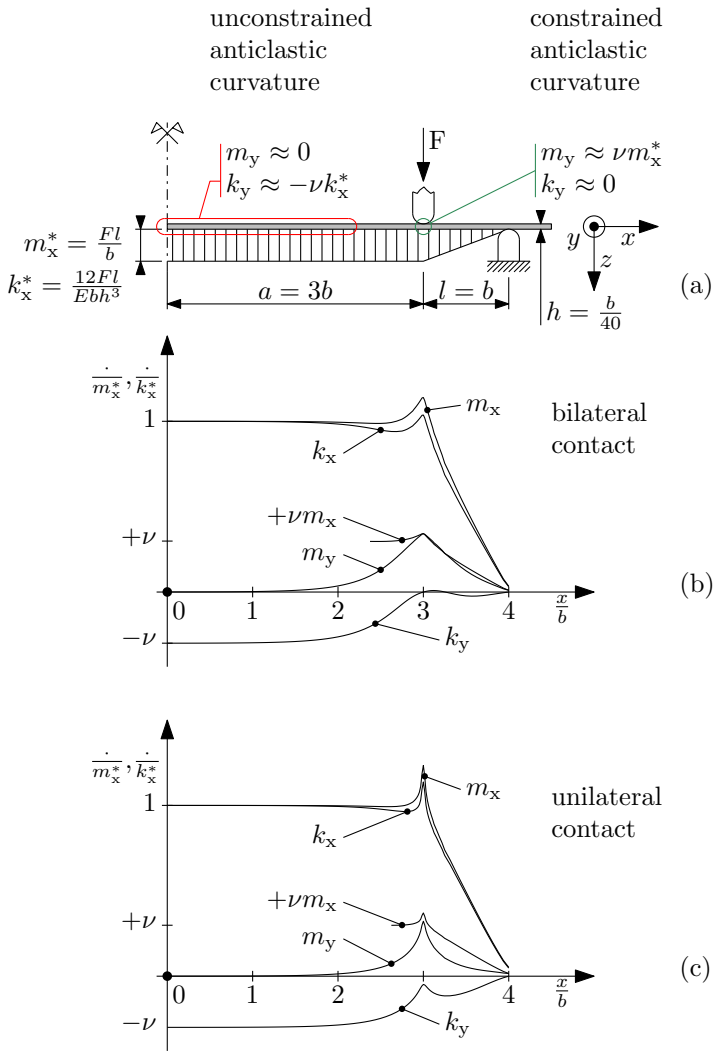

Figure 5: The *not-so-trivial* four point bending case, where b is the specimen out-of-sketch-plane width (we might call it *depth*). Moment fluxes and curvatures are sampled at the specimen midwidth, whereas they may vary while moving towards the flanks; the average value of m_x along the width must in fact coincide with m_x^* in correspondence with the load span.

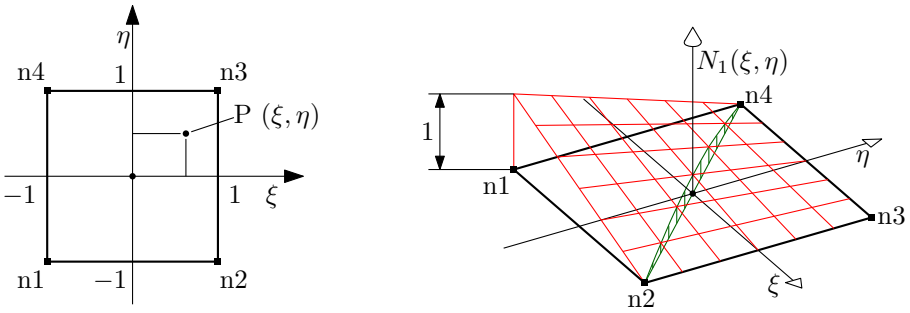

(a) (b)

Figure 6: Quadrilateral elementary domain (a), and a representative weight function (b).

0.2 Preliminary results

0.2.1 Interpolation functions for the quadrilateral domain

The elementary quadrilateral domain. A quadrilateral domain is considered whose vertices are conventionally located at the $(\pm 1, \pm 1)$ points of an adimensional (ξ, η) plane coordinate system, see Figure 6. Scalar values f_i are associated to a set of *nodal* points $\mathrm{P}_i \equiv [\xi_i, \eta_i]$, which for the present case coincide with the quadrangle vertices, numbered as in Figure.

A $f(\xi, \eta)$ interpolation function may be devised by defining a set of nodal influence functions $N_i(\xi, \eta)$ to be employed as the coefficients (weights) of a moving weighted average

$$f(\xi, \eta) \stackrel{\text{def}}{=} \sum_i N_i(\xi, \eta) f_i \tag{38}$$

Requisites for such weight functions are:

- for each point of the domain, the sum of the weights is unitary

$$\sum_i N_i(\xi, \eta) = 1, \ \forall [\xi, \eta] \tag{39}$$

- to grant continuity of the $f(\xi, \eta)$ function with the nodal samples, the influence of a node is unitary at its location, whereas the

influence of the others vanishes there, i.e.

$$N_i(\xi_j, \eta_j) = \delta_{ij} \tag{40}$$

where δ_{ij} is the Kronecker delta function.

Moreover, suitable functions should be continuous and straightforwardly differentiable up to any required degree.

Low order polynomials are ideal candidates for the application; for the particular domain, the nodal weight functions may be stated as

$$N_i(\xi, \eta) \stackrel{\text{def}}{=} \frac{1}{4} (1 \pm \xi) (1 \pm \eta), \tag{41}$$

where sign ambiguity is resolved for each i-th node by enforcing Eqn. 40.

The bilinear interpolation function defined by Eqs. 38 and 41 turns into a general linear relation with (ξ, η) if the four sample points (ξ_i, η_i, f_i) are coplanar – but otherwise arbitrary – in the ξ, η, f space.

Further generality may be introduced by *not* enforcing coplanarity.

The weight functions for the four-node quadrilateral are in fact quadratic although incomplete[20] in nature, due to the presence of the $\xi\eta$ product, and the absence of any ξ^2, η^2 term.

Each $N_i(\xi, \eta)$ term, and the combined $f(\xi, \eta)$ function, defined as in Eqn. 38, behave linearly if restricted to $\xi = \text{const.}$ or $\eta = \text{const.}$ loci – and in particular along the four edges; quadratic behaviour may instead arise along a general direction, e.g. along the diagonals, as in Fig. 6b example. Such behaviour is called *bilinear*.

We now consider the $f(\xi, \eta)$ interpolation function partial derivatives. The partial derivative

$$\frac{\partial f}{\partial \xi} = \underbrace{\left(\frac{f_2 - f_1}{2}\right)}_{[\Delta f / \Delta \xi]_{12}} \underbrace{\left(\frac{1 - \eta}{2}\right)}_{N_1 + N_2} + \underbrace{\left(\frac{f_3 - f_4}{2}\right)}_{[\Delta f / \Delta \xi]_{43}} \underbrace{\left(\frac{1 + \eta}{2}\right)}_{N_4 + N_3} = a\eta + b \tag{42}$$

linearly varies in η from the incremental ratio value measured at the $\eta = -1$ lower edge, to the value measured at the $\eta = 1$ upper edge; the other partial derivative

$$\frac{\partial f}{\partial \eta} = \left(\frac{f_4 - f_1}{2}\right) \left(\frac{1 - \xi}{2}\right) + \left(\frac{f_3 - f_2}{2}\right) \left(\frac{1 + \xi}{2}\right) = c\xi + d. \tag{43}$$

[20] or, equivalently, *enriched linear*, as discussed above and in the following

behaves similarly, with $c = a$. Partial derivatives in ξ, η remain constant while moving along the corresponding differentiation direction[21].

An equivalent expression for Eq. 38 is the following

$$f(\xi,\eta) = \begin{bmatrix} N_1(\xi,\eta) & \cdots & N_i(\xi,\eta) & \cdots & N_n(\xi,\eta) \end{bmatrix} \begin{bmatrix} f_1 \\ \vdots \\ f_i \\ \vdots \\ f_n \end{bmatrix}$$

$$= \underline{\underline{\mathrm{N}}}\,(\xi,\eta)\,\underline{\mathrm{f}}\,, \tag{44}$$

which resorts to the inner mechanics of the matrix-vector product for performing the summation; the $\underline{\mathrm{f}}$ vector collects the function nodal values, whereas the $\underline{\underline{\mathrm{N}}}\,(\xi,\eta)$ weigth function row matrix collects their influence coefficient at the provided (ξ,η) location.

The general planar quadrilateral domain. The interpolation functions introduced above for the natural quadrilateral may be profitably employed in defining a coordinate mapping between a general quadrangular domain – see Fig. 7a – and its reference counterpart, see Figures 6 or 7b.

In particular, we first define the $\underline{\xi}_i \mapsto \underline{\mathrm{x}}_i$ coordinate mapping for the four vertices[22] alone, where ξ, η are the reference (or natural, or elementary) coordinates and x, y are their physical counterpart.

Then, a mapping for the inner points may be derived by interpolation, namely

$$\underline{\mathrm{x}}\,\left(\underline{\xi}\right) = \underline{\mathrm{m}}\,\left(\underline{\xi}\right) = \sum_{i=1}^{4} N_i\left(\underline{\xi}\right)\,\underline{\mathrm{x}}_i, \tag{45}$$

or, by expliciting the $\underline{\mathrm{m}} \equiv \underline{\mathrm{x}}$ components,

$$\underline{\mathrm{m}}\,\left(\underline{\xi}\right) = \begin{bmatrix} x(\xi,\eta) \\ y(\xi,\eta) \end{bmatrix}$$

[21] The relevance of such partial derivative orders will appear clearer to the reader once the strain field will have been derived in paragraph XXX.

[22] The condensed notation $\underline{\xi}_i \equiv (\xi_i, \eta_i)$, $\underline{\mathrm{x}}_i \equiv (x_i, y_i)$ for coordinate vectors is employed.

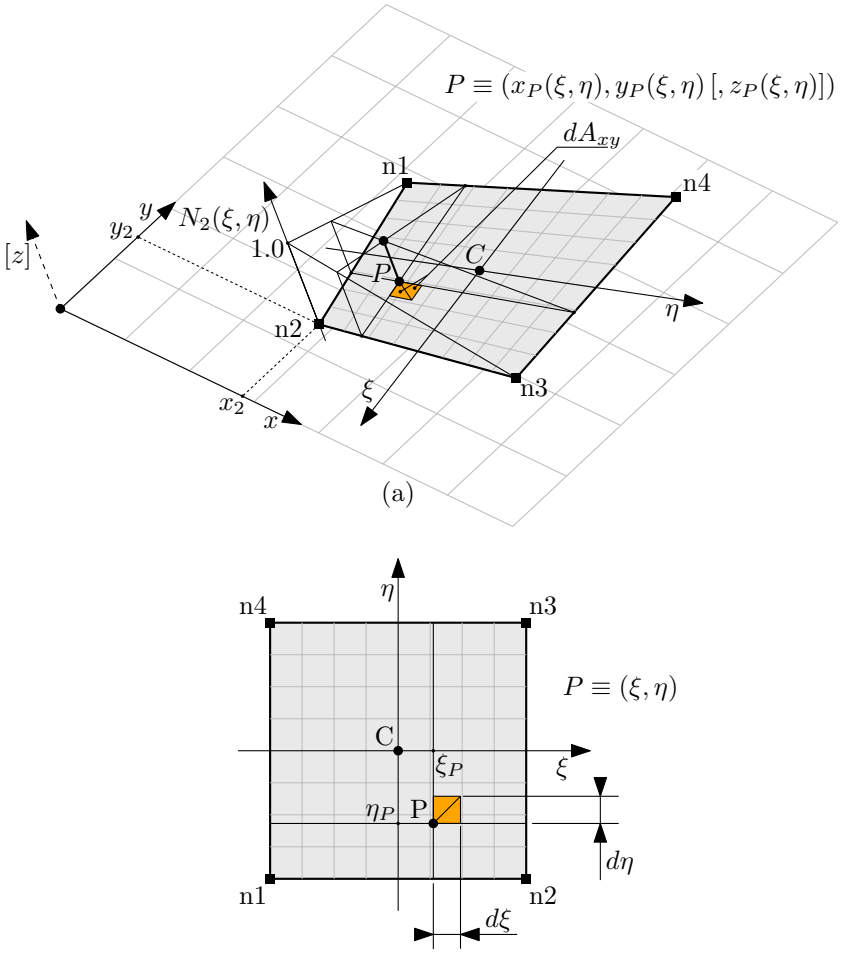

Figure 7: Quadrilateral general domain, (a), and its reference counterpart (b). If the general quadrangle is defined within a spatial environment, and not as a figure lying on the xy plane, limited z_i offsets are allowed at nodes with respect to such plane, which are not considered in Figure.

with

$$x(\xi,\eta) = \sum_{i=1}^{4} N_i(\xi,\eta) x_i \qquad\qquad y(\xi,\eta) = \sum_{i=1}^{4} N_i(\xi,\eta) y_i.$$

In the employed notation, the parametric dependence of the $\underline{\mathrm{m}}\,(\xi,\eta)$ mapping on the nodal coordinates is not explicit, but clearly unavoidable; the complete notation $\underline{\mathrm{m}}\,(\xi,\eta;\,\underline{\mathrm{x}}_i)$ might be alternatively employed, where $\underline{\mathrm{x}}_i$ is a placeholder for the physical coordinates of each node.

The availability of an inverse $\underline{\mathrm{m}}^{-1} : \underline{\mathrm{x}} \mapsto \underline{\xi}$ mapping is not granted; in particular, a closed form representation for such inverse is not generally available[23].

In the absence of an handy inverse mapping function, it is convenient to reinstate the interpolation procedure obtained for the natural domain, i.e.

$$f(\xi,\eta) \stackrel{\text{def}}{=} \sum_i N_i(\xi,\eta) f_i \tag{46}$$

The four f_i nodal values are interpolated based on the *natural* ξ,η coordinates of an inner P point, and not as a function of its physical x, y coordinates, that are never promoted to the independent variable role.

The interpolation scheme behind the $\underline{\mathrm{m}}$ mapping – and the mapping itself – behaves linearly along η =const. and ξ =const. one dimensional subdomains, and in particular along the quadrangle edges[24]; the inverse mapping $\underline{\mathrm{m}}^{-1}$ exists and it is a linear function[25] along the

[23] Inverse relations are derived in [5], which however are case-defined and based on a selection table; for a given $\bar{\underline{\mathrm{x}}}$ physical point, however, Newton-Raphson iterations rapidly converge to the $\bar{\underline{\xi}} = \underline{\mathrm{m}}^{-1}(\bar{\underline{\mathrm{x}}})$ solution if the centroid is chosen for algorithm initialization, see Section XXX

[24] see paragraph XXX

[25] A constructive proof may be defined for each edge as follows. We consider a generic Q point along such edge whose physical coordinates are (x_Q, y_Q). Of the two natural coordinates of Q, one is trivial to be derived since its value is constant along the edge. The other, for which we employ the λ placeholder symbol, may be defined through the expression

$$\lambda = 2\frac{(x_Q - x_i)(x_j - x_i) + (y_Q - y_i)(y_j - y_i)}{(x_j - x_i)^2 + (y_j - y_i)^2} - 1,$$

where i,j are the two subdomain endpoints at which λ equates -1 and $+1$, respec-

image of those line segments on the physical plane, under the further condition that its length is nonzero[26]. Being a composition of linear functions, the interpolation function $f(\underline{\mathrm{m}}^{-1}(x,y))$ is also linear along the aforementioned subdomains, and in particular along the quadrangle edges.

The directional derivatives of f with respect to x or y are obtained based the indirect relation

$$\begin{bmatrix} \frac{\partial f}{\partial \xi} \\ \frac{\partial f}{\partial \eta} \end{bmatrix} = \underbrace{\begin{bmatrix} \frac{\partial x}{\partial \xi} & \frac{\partial y}{\partial \xi} \\ \frac{\partial x}{\partial \eta} & \frac{\partial y}{\partial \eta} \end{bmatrix}}_{\underline{\underline{\mathrm{J}}}^{\top}(\xi,\eta;\underline{\mathrm{x}}_i)} \begin{bmatrix} \frac{\partial f}{\partial x} \\ \frac{\partial f}{\partial y} \end{bmatrix} \tag{47}$$

.

The function derivatives with respect to ξ, η are obtained as

$$\begin{bmatrix} \frac{\partial f}{\partial \xi} \\ \frac{\partial f}{\partial \eta} \end{bmatrix} = \sum_i \begin{bmatrix} \frac{\partial N_i}{\partial \xi} \\ \frac{\partial N_i}{\partial \eta} \end{bmatrix} f_i. \tag{48}$$

The *transposed* Jacobian matrix of the mapping function that appears in 47 is

$$\underline{\underline{\mathrm{J}}}^{\top}(\xi,\eta) = \begin{bmatrix} \frac{\partial x}{\partial \xi} & \frac{\partial y}{\partial \xi} \\ \frac{\partial x}{\partial \eta} & \frac{\partial y}{\partial \eta} \end{bmatrix} \tag{49}$$

$$= \sum_i \left(\begin{bmatrix} \frac{\partial N_i}{\partial \xi} & 0 \\ \frac{\partial N_i}{\partial \eta} & 0 \end{bmatrix} x_i + \begin{bmatrix} 0 & \frac{\partial N_i}{\partial \xi} \\ 0 & \frac{\partial N_i}{\partial \eta} \end{bmatrix} y_i \right) \tag{50}$$

If the latter matrix is assumed nonsingular – condition, this, that pairs the bijective nature of the $\underline{\mathrm{m}}$ mapping, equation 47 may be in-

tively, and $(x_i, y_i), (x_j, y_j)$ the associated physical coordinates. A similar function may be defined for any segment for which either ξ or η is constant, and not only for the quadrangle edges. Please note that the above inverse mapping formula is not applicable IIF the segment physical length at the denominator is zero.

[26]The case exists of an edge whose endpoints are superposed, i.e. the edge collapses to a point.

verted, thus leading to the form

$$\begin{bmatrix} \frac{\partial f}{\partial x} \\ \frac{\partial f}{\partial y} \end{bmatrix} = \left(\underline{\underline{\mathrm{J}}}^{\top} \right)^{-1} \begin{bmatrix} \cdots & \frac{\partial N_i}{\partial \xi} & \cdots \\ \cdots & \frac{\partial N_i}{\partial \eta} & \cdots \end{bmatrix} \begin{bmatrix} \vdots \\ f_i \\ \vdots \end{bmatrix} \tag{51}$$

$$= \underbrace{\left(\underline{\underline{\mathrm{J}}}^{\top} \right)^{-1} \begin{bmatrix} \frac{\partial \underline{\underline{\mathrm{N}}}}{\partial \xi} \\ \frac{\partial \underline{\underline{\mathrm{N}}}}{\partial \eta} \end{bmatrix}}_{\underline{\underline{\mathrm{L}}}(\xi,\eta;\underline{\mathrm{x}}_i), \text{ or just } \underline{\underline{\mathrm{L}}}(\xi,\eta)} \quad \underline{\mathrm{f}} \tag{52}$$

where the inner mechanics of the matrix-vector product are appointed for the Eq. 48 summation; the differential operator $\underline{\underline{\mathrm{L}}}(\xi, \eta; \underline{\mathrm{x}}_i)$ – or just $\underline{\underline{\mathrm{L}}}(\xi, \eta)$ if, again, we disregard its parametric dependence on the nodal coordinates – is also defined that extract the x, y directional derivatives of the interpolation function from its nodal values.

The general spatial quadrilateral domain. TODO.

0.2.2 Gaussian quadrature rules for some relevant domains.

Reference one dimensional domain. The gaussian quadrature rule for approximating the definite integral of a $f(\xi)$ function over the $[-1, 1]$ reference interval is constructed as the customary weighted sum of internal function samples, namely

$$\int_{-1}^{1} f(\xi) d\xi \approx \sum_{i=1}^{n} f(\xi_i) w_i; \tag{53}$$

Its peculiarity is to employ location-weight pairs (ξ_i, w_i) that are optimal with respect to the polynomial class of functions. Nevertheless, such choice has revealed itself to be robust enough for for a more general employment.

Let's consider a m-th order polynomial

$$p(\xi) \stackrel{\text{def}}{=} a_m \xi^m + a_{m-1} \xi^{m-1} + \ldots + a_1 \xi + a_0$$

whose exact integral is

$$\int_{-1}^{1} p(\xi) d\xi = \sum_{j=0}^{m} \frac{(-1)^j + 1}{j + 1} a_j$$

The integration residual between the exact definite integral and the weighted sample sum is defined as

$$r\left(a_j,(\xi_i,w_i)\right) \stackrel{\text{def}}{=} \sum_{i=1}^{n} p(\xi_i)w_i - \int_{-1}^{1} p(\xi)d\xi \tag{54}$$

The optimality condition is stated as follows: the quadrature rule involving n sample points (ξ_i, w_i), $i = 1 \dots n$ is optimal for the m-th order polynomial if a) the integration residual is null for general a_j values , and b) such condition does not hold for any lower-order sampling rule.

Once observed that the zero residual requirement is satisfied by any sampling rule if the polynomial a_j coefficients are all null, condition a) may be enforced by imposing that such zero residual value remains constant with varying a_j terms, i.e.

$$\begin{cases} \dfrac{\partial r\left(a_j,(\xi_i,w_i)\right)}{\partial a_j} = 0, \quad j = 0 \dots m \end{cases} \tag{55}$$

A system of $m+1$ polynomial equations of degree[27] $m+1$ is hence obtained in the $2n$ (ξ_i, w_i) unknowns; in the assumed absence of redundant equations, solutions do not exist if the constraints outnumber the unknowns, i.e. $m > 2n-1$. Limiting our discussion to the threshold condition $m = 2n-1$, an attentive algebraic manipulation of Eqns. 55 may be performed in order to extract the (ξ_i, w_i) solutions, which are unique apart from the pair permutations[28].

[27] the $(m+1)$-th order $w_m \xi^m$ term appears in equations

[28] In this note, location-weight pairs are obtained for the gaussian quadrature rule of order $n = 2$, aiming at illustrating the general procedure. The general $m = 2n-1 = 3$rd order polynomial is stated in the form

$$p(\xi) = a_3\xi^3 + a_2\xi^2 + a_1\xi + a_0, \quad \int_{-1}^{1} p(\xi)d\xi = \frac{2}{3}a_2 + 2a_0,$$

whereas the integral residual is

$$r = a_3\left(w_1\xi_1^3 + w_2\xi_2^3\right) + a_2\left(w_1\xi_1^2 + w_2\xi_2^2 - \frac{2}{3}\right) + a_1\left(w_1\xi_1 + w_2\xi_2\right) + a_0\left(w_1 + w_2 - 2\right)$$

Eqns 55 may be derived as

$$\begin{cases} 0 = \frac{\partial r}{\partial a_3} = w_1\xi_1^3 + w_2\xi_2^3 & (e_1) \\ 0 = \frac{\partial r}{\partial a_2} = w_1\xi_1^2 + w_2\xi_2^2 - \frac{2}{3} & (e_2) \\ 0 = \frac{\partial r}{\partial a_1} = w_1\xi_1 + w_2\xi_2 & (e_3) \\ 0 = \frac{\partial r}{\partial a_0} = w_1 + w_2 - 2 & (e_4) \end{cases}$$

n	ξ_i	w_i
1	0	2
2	$\pm\frac{1}{\sqrt{3}}$	1
3	0	$\frac{8}{9}$
	$\pm\sqrt{\frac{3}{5}}$	$\frac{5}{9}$
4	$\pm\sqrt{\frac{3}{7}-\frac{2}{7}\sqrt{\frac{6}{5}}}$	$\frac{18+\sqrt{30}}{36}$
	$\pm\sqrt{\frac{3}{7}+\frac{2}{7}\sqrt{\frac{6}{5}}}$	$\frac{18-\sqrt{30}}{36}$

Table 1: Integration points for the lower order gaussian quadrature rules.

Eqns. 55 solutions are reported in Table 1 for quadrature rules with up to $n = 4$ sample points[29].

It is noted that the integration points are symmetrically distributed with respect to the origin, and that the function is never sampled at the $\{-1, 1\}$ extremal points.

General one dimensional domain. The extension of the one dimensional quadrature rule from the reference domain $[-1, 1]$ to a general $[a, b]$ domain is pretty straightforward, requiring just a change of integration variable – i.e. a mapping function $x = m(\xi)$ s.t. $a = m(-1)$ and $b = m(1)$ – to obtain the following

$$\int_a^b g(x)dx = \int_{-1}^{1} g\left(m(\xi)\right) \frac{dm}{d\xi} d\xi \approx \sum_{i=1}^{n} g\left(m(\xi_i)\right) \left.\frac{dm}{d\xi}\right|_{\xi=\xi_i} w_i. \quad (56)$$

Such a mapping function may be conveniently defined along the same lines as the weight (or shape) function based interpolation, thus ob-

which are independent of the a_j coefficients.

By composing $\left(e_1 - \xi_1^2 e_3\right)/(w_2\xi_2)$ it is obtained that $\xi_2^2 = \xi_1^2$; e_2 may then be written as $(w_1 + w_2)\xi_1^2 = 2/3$, and then as $2\xi_1^2 = 2/3$, according to e_4. It derives that $\xi_{1,2} = \pm 1/\sqrt{3}$. Due to the opposite nature of the roots, e_3 implies $w_2 = w_1$, relation, this, that turns e_4 into $2w_1 = 2w_2 = 2$, and hence $w_{1,2} = 1$.

[29] see `https://pomax.github.io/bezierinfo/legendre-gauss.html` for higher order gaussian quadrature rule sample points.

taining

$$m(x) = \underbrace{\left(\frac{1-\xi}{2}\right)}_{N_1} a + \underbrace{\left(\frac{1+\xi}{2}\right)}_{N_2} b.$$

The first order derivative may be evaluated as

$$\frac{dm}{d\xi} = \frac{dN_1}{d\xi} a + \frac{dN_2}{d\xi} b = \frac{b-a}{2}$$

and it is constant along the interval, so that it may be collected outside of the summation, thus leading to

$$\int_a^b g(x)dx \approx \frac{b-a}{2} \sum_{i=1}^{n} g\left(\frac{b+a}{2} + \frac{b-a}{2}\xi_i\right) w_i. \tag{57}$$

Reference quadrangular domain. A quadrature rule for the reference quadrangular domain of Figure 6a may be derived by nesting the quadrature rule defined for the reference interval, see Eqn. 53, thus obtaining

$$\int_{-1}^{1}\int_{-1}^{1} f(\xi,\eta)\, d\xi d\eta \approx \sum_{i=1}^{p}\sum_{j=1}^{q} f(\xi_i,\eta_j)\, w_i w_j \tag{58}$$

where (ξ_i, w_i) and (η_j, w_j) are the coordinate-weight pairs of the two quadrature rules of p and q order, respectively, employed for spanning the two coordinate axes. The equivalent notation

$$\int_{-1}^{1}\int_{-1}^{1} f(\xi,\eta)\, d\xi d\eta \approx \sum_{l=1}^{pq} f\left(\underline{\xi}_l\right) w_l \tag{59}$$

emphasises the characteristic nature of the pq point/weight pairs for the domain and for the quadrature rule employed; a general integer bijection[30] $\{1 \dots pq\} \leftrightarrow \{1 \dots p\} \times \{1 \dots q\}$, $l \leftrightarrow (i,j)$ may be utilized

[30] e.g.

$$\{i-1; j-1\} = (l-1) \bmod (p,q), \quad l-1 = (j-1)q + (i-1)$$

where the operator

$$\{a_n; \dots; a_3; a_2; a_1\} = m \bmod (b_n, \dots, b_3, b_2, b_1)$$

consists in the extraction of the n least significant a_i digits of a mixed radix representation of the integer m with respect to the sequence of b_i bases, with $i = 1 \dots n$.

to formally derive the two-dimensional quadrature rule pairs

$$\underline{\xi}_{\,l} = (\xi_i, \eta_j)\,, \quad w_l = w_i w_j, \quad l = 1 \ldots pq \tag{60}$$

from their uniaxial counterparts.

General quadrangular domain. The rectangular infinitesimal area $dA_{\xi\eta} = d\xi d\eta$ in the neighborhood of a ξ_P, η_P location, see Figure 7b, is mapped to the dA_{xy} quadrangle of Figure 7a, which is composed by the two triangular areas

$$\begin{aligned} dA_{xy} = \quad & \frac{1}{2!}\begin{vmatrix} 1 & x\,(\xi_P & ,\eta_P &) & y\,(\xi_P & ,\eta_P &) \\ 1 & x\,(\xi_P + d\xi, & \eta_P &) & y\,(\xi_P + d\xi, & \eta_P &) \\ 1 & x\,(\xi_P + d\xi, & \eta_P + d\eta) & & y\,(\xi_P + d\xi, & \eta_P + d\eta) \end{vmatrix} + \\ & + \frac{1}{2!}\begin{vmatrix} 1 & x\,(\xi_P + d\xi, & \eta_P + d\eta) & & y\,(\xi_P + d\xi, & \eta_P + d\eta) \\ 1 & x\,(\xi_P & ,\eta_P + d\eta) & & y\,(\xi_P & ,\eta_P + d\eta) \\ 1 & x\,(\xi_P & ,\eta_P &) & y\,(\xi_P & ,\eta_P &) \end{vmatrix}. \end{aligned} \tag{61}$$

The determinant formula for the area of a triangle, shown below along with its n-dimensional symplex hypervolume generalization,

$$\mathcal{A} = \frac{1}{2!}\begin{vmatrix} 1 & x_1 & y_1 \\ 1 & x_2 & y_2 \\ 1 & x_3 & y_3 \end{vmatrix}, \quad \mathcal{H} = \frac{1}{n!}\begin{vmatrix} 1 & \underline{\mathrm{x}}_1 \\ 1 & \underline{\mathrm{x}}_2 \\ \vdots & \vdots \\ 1 & \underline{\mathrm{x}}_{n+1} \end{vmatrix} \tag{62}$$

has been employed above.

By operating a local multivariate linearization of the 61 matrix terms, the relation

$$\begin{aligned} dA_{xy} \approx \quad & \frac{1}{2!}\begin{vmatrix} 1 & x & y \\ 1 & x + x_{,\xi} d\xi & y + y_{,\xi} d\xi \\ 1 & x + x_{,\xi} d\xi + x_{,\eta} d\eta & y + y_{,\xi} d\xi + y_{,\eta} d\eta \end{vmatrix} + \\ & + \frac{1}{2!}\begin{vmatrix} 1 & x + x_{,\xi} d\xi + x_{,\eta} d\eta & y + y_{,\xi} d\xi + y_{,\eta} d\eta \\ 1 & x + x_{,\eta} d\eta & y + y_{,\eta} d\eta \\ 1 & x & y \end{vmatrix} \end{aligned}$$

is obtained, where $x, y, x_{,\xi}, x_{,\eta}, y_{,\xi}$, and $y_{,\eta}$ are the x, y functions and their first order partial derivatives, evaluated at the (ξ_P, η_P) point; infinitesimal terms of order higher than $d\xi, d\eta$ are neglected.

After some matrix manipulations[31], the following expression is obtained

$$dA_{xy} = \underbrace{\begin{vmatrix} x_{,\xi} & y_{,\xi} \\ x_{,\eta} & y_{,\eta} \end{vmatrix}}_{\left|J^{\mathrm{T}}(\xi_P,\eta_P;\underline{\mathrm{x}},\underline{\mathrm{y}})\right|} dA_{\xi\eta} \tag{63}$$

that equates the ratio of the mapped and of the reference areas to the determinant of the transformation (transpose) Jacobian matrix[32].

After the preparatory passages above, we obtain

$$\iint_{A_{xy}} g(x,y)dA_{xy} = \int_{-1}^{1}\int_{-1}^{1} g\left(x\left(\xi,\eta\right), y\left(\xi,\eta\right)\right)\left|J(\xi,\eta)\right| d\xi d\eta, \tag{64}$$

thus reducing the quadrature over a general domain to its reference domain counterpart, which has been discussed in the paragraph above.

Based on Eqn. 59, the quadrature rule

$$\iint_{A_{xy}} g(\underline{\mathrm{x}})dA_{xy} \approx \sum_{l=1}^{pq} g\left(\underline{\mathrm{x}}\left(\underline{\xi}_l\right)\right)\left|J(\underline{\xi}_l)\right| w_l \tag{65}$$

[31] In the first determinant, the second row is subtracted from the third one, and the first row is subtracted from the second one. The $d\xi$, $d\eta$ factors are then collected from the second and the third row respectively. In the second determinant, the second row is subtracted from the first one, and the third row is subtracted from the second one. The $d\xi$, $d\eta$ factors are then collected from the first and the second row respectively. We now have

$$dA_{xy} = \frac{1}{2}\begin{vmatrix} 1 & x & y \\ 0 & x_{,\xi} & y_{,\xi} \\ 0 & x_{,\eta} & y_{,\eta} \end{vmatrix} d\xi d\eta + \frac{1}{2}\begin{vmatrix} 0 & x_{,\xi} & y_{,\xi} \\ 0 & x_{,\eta} & y_{,\eta} \\ 1 & x & y \end{vmatrix} d\xi d\eta$$

The first column of both the determinants contains a single, unitary, nonzero term, whose row and column indexes are even once added up; the determinants of the associated complementary minors hence equate their whole matrix counterpart. We hence obtain

$$dA_{xy} = \frac{1}{2}\begin{vmatrix} x_{,\xi} & y_{,\xi} \\ x_{,\eta} & y_{,\eta} \end{vmatrix} d\xi d\eta + \frac{1}{2}\begin{vmatrix} x_{,\xi} & y_{,\xi} \\ x_{,\eta} & y_{,\eta} \end{vmatrix} d\xi d\eta$$

from which Eq.63 may be straightforwardly derived.

[32] The Jacobian matrix for a general $\underline{\xi} \mapsto \underline{\mathrm{x}}$ mapping is in fact defined according to

$$[J(\underline{\xi}_P)]_{ij} \stackrel{\mathrm{def}}{=} \left.\frac{\partial x_i}{\partial \xi_j}\right|_{\underline{\xi}=\underline{\xi}_P} \qquad i,j = 1\ldots n$$

being i the generic matrix term row index, and j the column index

is derived, stating that the definite integral of a g integrand over a quadrangular domain pertaining to the physical x, y plane (x, y are dimensional quantities, namely lengths) may be approximated as follows:

1. a reference-to-physical domain mapping is defined, that is based on the vertex physical coordinate interpolation;

2. the function is sampled at the physical locations that are the images of the Gaussian integration points previously obtained for the reference domain;

3. a weighted sum of the collected samples is performed, where the weights consist in the product of i) the adimensional w_l Gauss point weight (suitable for integrating on the reference domain), and ii) a dimensional area scaling term, that equals the determinant of the transformation Jacobian matrix, locally evaluated at the Gauss points.

0.3 The bilinear isoparametric shear-deformable shell element

> This is a four-node, thick-shell element with global displacements and rotations as degrees of freedom. Bilinear interpolation is used for the coordinates, displacements and the rotations. The membrane strains are obtained from the displacement field; the curvatures from the rotation field. The transverse shear strains are calculated at the middle of the edges and interpolated to the integration points. In this way, a very efficient and simple element is obtained which exhibits correct behavior in the limiting case of thin shells. The element can be used in curved shell analysis as well as in the analysis of complicated plate structures. For the latter case, the element is easy to use since connections between intersecting plates can be modeled without tying. Due to its simple formulation when compared to the standard higher order shell elements, it is less expensive and, therefore, very attractive in nonlinear analysis. The element is not very sensitive to distortion, particularly if the corner nodes lie in the same plane. All constitutive relations can be used with this element.
>
> — MSC.Marc 2013.1 Documentation, vol. B, Element library.

0.3.1 Element geometry

Once introduced the required algebraic paraphernalia, the definition of a quadrilateral bilinear isoparametric shear-deformable shell element is straightforward.

The quadrilateral element geometry is defined by the position in space of its four vertices, which constitute the set of *nodal points*, or *nodes*, i.e. the set of locations at which field components are primarily, parametrically, defined; interpolation is employed in deriving the field values elsewhere.

A suitable interpolation scheme, named *bilinear*, has been introduced in paragraph 0.2.1; the related functions depend on the normalized coordinate pair $\xi, \eta \in [-1, 1]$ that spans the elementary quadrilateral of Figure 6.

A global reference system OXYZ is employed for concurrently dealing with multiple elements (i.e. at a whole model scale); a more convenient, local Cxyz reference system, z being locally normal to the shell, is used when a single element is under scrutiny – e.g. in the current paragraph.

Nodal coordinates define the element initial, undeformed, geometry[33], or, alternatively, the portion of thin-walled body reference surface that pertains to the current element; physical, spatial coordinates for each other element point may be retrieved by interpolation based on the associated pair of natural ξ, η coordinates, namely

$$\begin{bmatrix} X(\xi,\eta) \\ Y(\xi,\eta) \\ Z(\xi,\eta) \end{bmatrix} = \sum_{i=1}^{n} N_i(\xi,\eta) \begin{bmatrix} X_i \\ Y_i \\ Z_i \end{bmatrix}, \quad \begin{bmatrix} x(\xi,\eta) \\ y(\xi,\eta) \\ z(\xi,\eta) \end{bmatrix} = \sum_{i=1}^{n} N_i(\xi,\eta) \begin{bmatrix} x_i \\ y_i \\ z_i \end{bmatrix} \quad (66)$$

with reference to both the global and the local systems.

In particular, the C centroid is the image within the physical space of the $\xi = 0, \eta = 0$ natural coordinate system origin.

The in-plane orientation of the local Cxyz reference system is somewhat arbitrary and implementation-specific; the MSC.Marc approach is used as an example, and it is described in the following. The in-plane x, y axes are tentatively defined[34] based on the physical directions that are associated with the ξ, η natural axes, i.e. the oriented segments spanning a) from the midpoint of the n4-n1 edge to the midpoint of the n2-n3 edge, and b) from the midpoint of the n1-n2 edge to the midpoint of the n3-n4 edge, respectively; however, these two tentative axes are not mutually orthogonal in general. The mutual Cxy angle is then amended by rotating those interim axes with respect to a third, binormal axis Cz, while preserving their initial bisectrix.

[33] They are however continuosly updated within most common nonlinear analysis frameworks, where *initial* usually refers to the last computed, aka *previous* step of an iterative scheme.

[34] The MSC.Marc element library documentation defines them as a normalized form of the

$$\left(\frac{\partial X}{\partial \xi}, \frac{\partial Y}{\partial \xi}, \frac{\partial Z}{\partial \xi},\right)\Big|_{\xi=0,\eta=0}, \left(\frac{\partial X}{\partial \eta}, \frac{\partial Y}{\partial \eta}, \frac{\partial Z}{\partial \eta},\right)\Big|_{\xi=0,\eta=0},$$

vectors, which are evaluated at the centroid. The two definitions may be proved equivalent based on the bilinear interpolation properties.

The resulting quadrilateral shell element has limited capabilities of representing a curve surface; it is in fact flat, apart from a (suggestedly limited) anticlastic curvature of the element diagonals, which is associated to the quadratic $\xi\eta$ term of the interpolation functions. It is e.g. not capable of representing a single curvature surface.

The curve nature of a thin-walled body midsurface may thus be reproduced by recurring to a tessellation of essentially flat, but mutually angled elements.

0.3.2 Displacement and rotation fields

The element degrees of freedom consist in the displacements and the rotations of the four quadrilateral vertices, i.e. *nodes*.

By interpolating the nodal values, displacement and rotation functions may be derived along the element as

$$\begin{bmatrix} u(\xi,\eta) \\ v(\xi,\eta) \\ w(\xi,\eta) \end{bmatrix} = \sum_{i=1}^{4} N_i(\xi,\eta) \begin{bmatrix} u_i \\ v_i \\ w_i \end{bmatrix} \tag{67}$$

$$\begin{bmatrix} \theta(\xi,\eta) \\ \phi(\xi,\eta) \\ \psi(\xi,\eta) \end{bmatrix} = \sum_{i=1}^{4} N_i(\xi,\eta) \begin{bmatrix} \theta_i \\ \phi_i \\ \psi_i \end{bmatrix} \tag{68}$$

with $i = 1 \dots 4$ cycling along the element nodes. If we collect the element nodal degree of freedom (DOF)s within the six column vectors

$$\underline{\mathrm{u}} = \begin{bmatrix} \vdots \\ u_i \\ \vdots \end{bmatrix} \qquad \underline{\mathrm{v}} = \begin{bmatrix} \vdots \\ v_i \\ \vdots \end{bmatrix} \qquad \underline{\mathrm{w}} = \begin{bmatrix} \vdots \\ w_i \\ \vdots \end{bmatrix}$$

$$\underline{\theta} = \begin{bmatrix} \vdots \\ \theta_i \\ \vdots \end{bmatrix} \qquad \underline{\phi} = \begin{bmatrix} \vdots \\ \phi_i \\ \vdots \end{bmatrix} \qquad \underline{\psi} = \begin{bmatrix} \vdots \\ \psi_i \\ \vdots \end{bmatrix}$$

we may resort to compact notations in the form

$$u(\xi,\eta) = \underline{\underline{\mathrm{N}}}\,(\xi,\eta)\,\underline{\mathrm{u}} \qquad\qquad v(\xi,\eta) = \underline{\underline{\mathrm{N}}}\,(\xi,\eta)\,\underline{\mathrm{v}}$$

et cetera.

Those column vectors are in turn stacked to form the cumulative

$$\underline{\mathrm{d}}^{\top} = \begin{bmatrix} \underline{\mathrm{u}}^{\top} & \underline{\mathrm{v}}^{\top} & \underline{\mathrm{w}}^{\top} & \underline{\theta}^{\top} & \underline{\phi}^{\top} & \underline{\psi}^{\top} \end{bmatrix} \tag{69}$$

DOF column vector for the title element.

The $\underline{\psi}$ vector associated with the drilling degree of freedom – i.e. the rotation with respect to the normal z axis – is *not* omitted, although its contribution to the element strain energy deserves some discussion, see the dedicated paragraph below.

0.3.3 Strains

By recalling Eqn. 51, we have e.g.

$$\begin{bmatrix} \frac{\partial u}{\partial x} \\ \frac{\partial u}{\partial y} \end{bmatrix} = \underbrace{\left(\underline{\underline{\mathrm{J}}}'\right)^{-1} \begin{bmatrix} \cdots & \frac{\partial N_i}{\partial \xi} & \cdots \\ \cdots & \frac{\partial N_i}{\partial \eta} & \cdots \end{bmatrix}}_{\underline{\underline{\mathrm{L}}}(\xi,\eta;\underline{\mathrm{x}}_i) \text{ or just } \underline{\underline{\mathrm{L}}}(\xi,\eta)} \begin{bmatrix} \vdots \\ u_i \\ \vdots \end{bmatrix} \tag{70}$$

for the x-oriented displacement component; the differential operator $\underline{\mathrm{L}}(\xi, \eta; \underline{\mathrm{x}}_i)$, which extracts the x, y directional derivatives from the nodal values of a given field component, is employed.

A block defined $Q(\xi, \eta)$ matrix is thus obtained that cumulatively relates the in-plane displacement component derivatives to the associated nodal values

$$\begin{bmatrix} \frac{\partial u}{\partial x} \\ \frac{\partial u}{\partial y} \\ \frac{\partial v}{\partial x} \\ \frac{\partial v}{\partial y} \end{bmatrix} = \underbrace{\begin{bmatrix} \underline{\underline{\mathrm{L}}}(\xi,\eta) & \underline{\underline{0}} \\ \underline{\underline{0}} & \underline{\underline{\mathrm{L}}}(\xi,\eta) \end{bmatrix}}_{\underline{\underline{\mathrm{Q}}}(\xi,\eta)} \begin{bmatrix} \underline{\mathrm{u}} \\ \underline{\mathrm{v}} \end{bmatrix} \tag{71}$$

An equivalent relation may then be obtained for the rotation field

$$\begin{bmatrix} \frac{\partial \theta}{\partial x} \\ \frac{\partial \theta}{\partial y} \\ \frac{\partial \phi}{\partial x} \\ \frac{\partial \phi}{\partial y} \end{bmatrix} = \underline{\underline{\mathrm{Q}}}(\xi,\eta) \begin{bmatrix} \underline{\theta} \\ \underline{\phi} \end{bmatrix} \tag{72}$$

By making use of two auxiliary matrices $\underline{\underline{\mathrm{H}}}'$ and $\underline{\underline{\mathrm{H}}}''$ that collect the $\{0, \pm 1\}$ coefficients in Eqns. 10 and 11, we obtain that the IP

strain components at the reference surface, and the curvatures equate respectively

$$\begin{bmatrix} e_x \\ e_y \\ g_{xy} \end{bmatrix} = \underbrace{\begin{bmatrix} +1 & 0 & 0 & 0 \\ 0 & 0 & 0 & +1 \\ 0 & +1 & +1 & 0 \end{bmatrix}}_{\underline{\underline{\mathrm{H}}}'} \begin{bmatrix} \frac{\partial u}{\partial x} \\ \frac{\partial u}{\partial y} \\ \frac{\partial v}{\partial x} \\ \frac{\partial v}{\partial y} \end{bmatrix} = \underline{\underline{\mathrm{H}}}' \, \underline{\underline{\mathrm{Q}}}(\xi, \eta) \begin{bmatrix} \underline{\mathrm{u}} \\ \underline{\mathrm{v}} \end{bmatrix} \tag{73}$$

$$\begin{bmatrix} \kappa_x \\ \kappa_y \\ \kappa_{xy} \end{bmatrix} = \underbrace{\begin{bmatrix} 0 & 0 & +1 & 0 \\ 0 & -1 & 0 & 0 \\ -1 & 0 & 0 & +1 \end{bmatrix}}_{\underline{\underline{\mathrm{H}}}''} \begin{bmatrix} \frac{\partial \theta}{\partial x} \\ \frac{\partial \theta}{\partial y} \\ \frac{\partial \phi}{\partial x} \\ \frac{\partial \phi}{\partial y} \end{bmatrix} = \underline{\underline{\mathrm{H}}}'' \, \underline{\underline{\mathrm{Q}}}(\xi, \eta) \begin{bmatrix} \underline{\theta} \\ \underline{\phi} \end{bmatrix} \tag{74}$$

or, by referring to the whole set of nodal DOFs,

$$\underline{\mathrm{e}} = \underbrace{\begin{bmatrix} \underline{\underline{\mathrm{H}}}' \, \underline{\underline{\mathrm{Q}}}(\xi, \eta) & \underline{\underline{0}} & \underline{\underline{0}} & \underline{\underline{0}} & \underline{\underline{0}} \end{bmatrix}}_{\underline{\underline{\mathrm{B}}}_e(\xi, \eta)} \underline{\mathrm{d}} \tag{75}$$

$$\underline{\kappa} = \underbrace{\begin{bmatrix} \underline{\underline{0}} & \underline{\underline{0}} & \underline{\underline{0}} & \underline{\underline{\mathrm{H}}}'' \, \underline{\underline{\mathrm{Q}}}(\xi, \eta) & \underline{\underline{0}} \end{bmatrix}}_{\underline{\underline{\mathrm{B}}}_\kappa(\xi, \eta)} \underline{\mathrm{d}} \, . \tag{76}$$

The $\underline{\underline{\mathrm{B}}}_e$ and $\underline{\underline{\mathrm{B}}}_\kappa$ matrices are block-defined by appending to the 3x8 blocks introduced in Eqn. 73 and 74, respectively, a suitable set of 3x3 null block placeholders.

The IP strain components at a generico ξ, η, z point along the element thickness may then be derived according to Eqn. 12 as a (linear) function of the nodal degrees of freedom

$$\underline{\epsilon}(\xi, \eta, z) = \left(\underline{\underline{\mathrm{B}}}_e(\xi, \eta) + z \, \underline{\underline{\mathrm{B}}}_\kappa(\xi, \eta) \right) \underline{\mathrm{d}} \, ; \tag{77}$$

the OOP shear strain components, as defined in Eqns. 4 and 5, become instead

$$\begin{bmatrix} \bar{\gamma}_{zx} \\ \bar{\gamma}_{yz} \end{bmatrix} = \underline{\underline{\mathrm{L}}}(\xi, \eta) \, \underline{\mathrm{w}} + \begin{bmatrix} 0 & +\underline{\underline{\mathrm{N}}}(\xi, \eta) \\ -\underline{\underline{\mathrm{N}}}(\xi, \eta) & 0 \end{bmatrix} \begin{bmatrix} \underline{\theta} \\ \underline{\phi} \end{bmatrix}, \tag{78}$$

and thus, by employing a notation consistent with **??**,

$$\begin{bmatrix} \bar{\gamma}_{zx} \\ \bar{\gamma}_{yz} \end{bmatrix} = \underbrace{\begin{bmatrix} \underline{\underline{0}} & \underline{\underline{0}} & \underline{\underline{\mathrm{L}}}(\xi, \eta) & 0 & \underline{\underline{\mathrm{N}}}(\xi, \eta) & \underline{\underline{0}} \\ \underline{\underline{0}} & \underline{\underline{0}} & \underline{\underline{\mathrm{L}}}(\xi, \eta) & -\underline{\underline{\mathrm{N}}}(\xi, \eta) & 0 & \underline{\underline{0}} \end{bmatrix}}_{\underline{\underline{\mathrm{B}}}_\gamma(\xi, \eta)} \underline{\mathrm{d}} \tag{79}$$

where the transformation matrix that derives the out-of-plane, interlaminar strains from the nodal degrees of freedom vector is constituted by five 2×4 blocks.

0.3.4 Stresses

In general, material constitutive laws are employed in deriving stress components from their strain counterpart.

In the case of a shell element, the plane stress relations discussed in Paragraph 0.1, see Eqns. 13, may be employed in deriving the pointwise IP stress components from the associated strains.

Also, the plate constitutive laws reported as Eqns. 19 may be employed in deriving the TT force and moment IP stress resultants from the generalized strains obtained in Eqns. 75, 76. The OOP shear stress resultants may be derived from the associated Eqns. 79 generalized strains by resorting to Eq. 24.

0.3.5 The element stiffness matrix.

In this paragraph, the elastic behaviour of the finite element under scrutiny is derived.

The element is considered in its deformed configuration, being

$$\underline{\mathrm{d}}^{\top} = \begin{bmatrix} \underline{\mathrm{u}}^{\top} & \underline{\mathrm{v}}^{\top} & \underline{\mathrm{w}}^{\top} & \underline{\theta}^{\top} & \underline{\phi}^{\top} & \underline{\psi}^{\top} \end{bmatrix} \tag{80}$$

the DOF vector associated with such condition.

A virtual displacement field perturbs such deformed configuration; as usual, those virtual displacements are infinitesimal, they do occur while time is held constant, and, being otherwise arbitrary, they respect the existing kinematic constraints.

Whilst, in fact, no external constrains are applied to the element, the motion of the pertaining material points is prescribed based on a) the assumed plate kinematics, and b) on the bilinear, isoparametric interpolation laws that propagate the generalized nodal displacements $\delta\underline{\mathrm{d}}$ towards the quadrilateral's interior.

Since the element is supposed to elastically react to such $\underline{\mathrm{d}}$ deformed configuration, a set of external actions

$$\underline{\mathrm{G}}^{\top} = \begin{bmatrix} \underline{\mathrm{U}}^{\top} & \underline{\mathrm{V}}^{\top} & \underline{\mathrm{W}}^{\top} & \underline{\Theta}^{\top} & \underline{\Phi}^{\top} & \underline{\Psi}^{\top} \end{bmatrix} \tag{81}$$

is applied at nodes[35] – one each DOF, that equilibrate the stretched element reactions.

[35] There is no lack of generality in assuming the equilibrating external actions applied at DOFs only, as discussed in Par. XXX below.

The nature of each $\underline{\mathrm{G}}$ generalized force component is defined based on the nature of the associated generalized displacement, such that the overall virtual work they perform on any $\delta\underline{\mathrm{d}}$ motion is

$$\delta\Upsilon_{\mathrm{e}} = \delta\underline{\mathrm{d}}^{\top}\,\underline{\mathrm{G}}\,. \tag{82}$$

Let's now consider the internal virtual work produced by the same $\delta\underline{\mathrm{d}}$ displacements.

The IP stress components that are induced by the $\underline{\mathrm{d}}$ generalized displacements equal

$$\underline{\sigma} \;=\; \underline{\underline{\mathrm{D}}}\,(z)\,\big(\underline{\underline{\mathrm{B}}}_{e}(\xi,\eta) + \underline{\underline{\mathrm{B}}}_{\kappa}(\xi,\eta)z\big)\;\underline{\mathrm{d}} \tag{83}$$

according to the previous paragraphs,and they perform [volumic density of] internal work on the

$$\delta\underline{\epsilon} \;=\; \big(\underline{\underline{\mathrm{B}}}_{e}(\xi,\eta) + \underline{\underline{\mathrm{B}}}_{\kappa}(\xi,\eta)z\big)\,\delta\underline{\mathrm{d}} \tag{84}$$

virtual elongations.

Similar considerations may be assessed with reference to the plate theory framework; in particular, the internal action stress and moment resultants may be derived from the element DOF as

$$\underline{\mathrm{q}} \;=\; \big(\underline{\mathrm{a}}\;\underline{\underline{\mathrm{B}}}_{e}(\xi,\eta) + \underline{\mathrm{b}}\;\underline{\underline{\mathrm{B}}}_{\kappa}(\xi,\eta)\big)\;\underline{\mathrm{d}} \tag{85}$$

$$\underline{\mathrm{m}} \;=\; \big(\underline{\mathrm{b}}^{\top}\,\underline{\underline{\mathrm{B}}}_{e}(\xi,\eta) + \underline{\mathrm{c}}\;\underline{\underline{\mathrm{B}}}_{\kappa}(\xi,\eta)\big)\;\underline{\mathrm{d}}\,, \tag{86}$$

and they perform [surficial density of] virtual work on the virtual variation of the generalized strain components

$$\delta\underline{\mathrm{e}} \;=\; \underline{\underline{\mathrm{B}}}_{e}(\xi,\eta)\delta\underline{\mathrm{d}} \tag{87}$$

$$\delta\underline{\kappa} \;=\; \underline{\underline{\mathrm{B}}}_{\kappa}(\xi,\eta)\delta\underline{\mathrm{d}}\,, \tag{88}$$

The associated internal virtual work may be derived by integration along the element volume, i.e. along the thickness, and along the quadrilateral portion of reference surface that pertains to the element. We thus obtain a first contribution to the overall internal virtual work

$$\begin{aligned}
\delta\Upsilon_{\mathrm{i}}^{\dagger} &= \iint_{\mathcal{A}}\int_{h} \delta\underline{\epsilon}^{\top}\,\underline{\sigma}\,dz d\mathcal{A} \\
&= \iint_{\mathcal{A}}\int_{h} \big(\big(\underline{\underline{\mathrm{B}}}_{e} + \underline{\underline{\mathrm{B}}}_{\kappa}z\big)\,\delta\underline{\mathrm{d}}\big)^{\top}\;\underline{\underline{\mathrm{D}}}\;\big(\underline{\underline{\mathrm{B}}}_{e} + \underline{\underline{\mathrm{B}}}_{\kappa}z\big)\;\underline{\mathrm{d}}\,dz d\mathcal{A} \\
&= \delta\underline{\mathrm{d}}^{\top}\left[\iint_{\mathcal{A}}\int_{h} \big(\underline{\underline{\mathrm{B}}}_{e}^{\top} + \underline{\underline{\mathrm{B}}}_{\kappa}^{\top}z\big)\;\underline{\underline{\mathrm{D}}}\;\big(\underline{\underline{\mathrm{B}}}_{e} + \underline{\underline{\mathrm{B}}}_{\kappa}z\big)\,dz d\mathcal{A}\right]\;\underline{\mathrm{d}} \\
&= \delta\underline{\mathrm{d}}^{\top}\,\underline{\underline{\mathrm{K}}}^{\dagger}\,\underline{\mathrm{d}}\,,
\end{aligned} \tag{89}$$

which may equivalently be expressed based on the plate/laminate constitutive matrix minors as

$$\begin{aligned}\delta\Upsilon_{\mathrm{i}}^{\dagger} &= \iint_{\mathcal{A}} \left(\delta\underline{\mathrm{e}}^{\top}\,\underline{\mathrm{q}} + \delta\underline{\kappa}^{\top}\,\underline{\mathrm{m}}\right) d\mathcal{A} \\ &= \delta\underline{\mathrm{d}}^{\top}\left[\iint_{\mathcal{A}} \left(\underline{\underline{\mathrm{B}}}_{e}^{\top}\left(\underline{\underline{\mathrm{a}}}\,\underline{\underline{\mathrm{B}}}_{e} + \underline{\underline{\mathrm{b}}}\,\underline{\underline{\mathrm{B}}}_{\kappa}\right) + \underline{\underline{\mathrm{B}}}_{\kappa}^{\top}\left(\underline{\underline{\mathrm{b}}}\,\underline{\underline{\mathrm{B}}}_{e} + \underline{\underline{\mathrm{c}}}\,\underline{\underline{\mathrm{B}}}_{\kappa}\right)\right) d\mathcal{A}\right]\,\underline{\mathrm{d}} \\ &= \delta\underline{\mathrm{d}}^{\top}\,\underline{\underline{\mathrm{K}}}_{\sigma}\,\underline{\mathrm{d}}\,, \end{aligned} \tag{90}$$

since we recall that

$$\left\{\underline{\underline{\mathrm{a}}}\,,\,\underline{\underline{\mathrm{b}}}\,,\,\underline{\underline{\mathrm{c}}}\right\} = \int_{h} \underline{\underline{\mathrm{D}}}\,\left\{1, z, z^{2}\right\} dz,$$

and that the $\underline{\underline{\mathrm{B}}}_{\{e,\kappa\}}$ matrices are constant in z.

Integration along i) the reference surface, and ii) along the thickness is numerically performed through potentially distinct quadrature rules; in particular, contributions are collected along the surface according to the two points per axis (four points overall) Gaussian quadrature formula introduced in Par. 0.2.2, whilst a (composite) Simpson rule is applied in z, being each material layer sampled at its outer and middle points. In general, any volume integral along the element, i.e.

$$\begin{aligned}&\iiint_{\Omega} g(\xi,\eta,x,y,z)d\Omega = \\ &= \int_{-1}^{+1}\int_{-1}^{+1}\int_{-\frac{h}{2}+o}^{+\frac{h}{2}+o} g(\xi,\eta,x(\xi,\eta),y(\xi,\eta),z)dz\,\left|\,\underline{\mathrm{J}}\,(\xi,\eta)\right|\,d\xi d\eta,\end{aligned} \tag{91}$$

where g is a generic function of the isoparametric or physical coordinates, will be numerically performed according to such scheme.

the outer integrals in the isoparametric coordinates (ξ,η) are evaluated according to the usual two points per axis gaussian quadrature rule, whereas a [composite] Simpson rule is employed along the TT coordinate z.

The two points per axis quadrature rule is the lowest order rule that returns an exact integral evaluation in the case of *distortion-free*[36] elements, i.e. planar elements whose peculiar (parallelogram) shape also

[36] Many distinct definitions are associated to the element distortion concept, being the one reported relevant for the specific dissertation passage.

determines a linear (vs. bilinear) isoparametric mapping. Since the associated Jacobian matrix is constant with respect to ξ, η, the $\underline{\underline{\mathrm{L}}}$ matrix defined in 70 linearly varies with such isoparametric coordinates, and so do the $\underline{\underline{\mathrm{B}}}_e$, $\underline{\underline{\mathrm{B}}}_\kappa$ matrices. The integrand of Eqn. 89 is thus a quadratic function of the ξ, η integration variables, as the Jacobian matrix determinant that scales the physical and the natural infinitesimal areas, see Eq. 63, is also constant.

A second contribution to the internal virtual work, which is due to the out-of-plane shear components, may be obtained with similar considerations based on Eqns. 79 and 23; such contribution may be cast as

$$\begin{aligned}
\delta\Upsilon_{\mathrm{i}}^{\ddagger} &= \iint_{\mathcal{A}} \delta\underline{\gamma}_z^{\top}\, \underline{\mathrm{q}}_z d\mathcal{A} \\
&= \delta\underline{\mathrm{d}}^{\top} \left[h \iint_{\mathcal{A}} \underline{\underline{\mathrm{B}}}_\gamma^{\top}\, \underline{\underline{\Gamma}}\, \underline{\underline{\mathrm{B}}}_\gamma d\mathcal{A} \right] \underline{\mathrm{d}} \\
&= \delta\underline{\mathrm{d}}^{\top}\, \underline{\underline{\mathrm{K}}}_\gamma\, \underline{\mathrm{d}}\,. \qquad (92)
\end{aligned}$$

The overall internal work is thus

$$\begin{aligned}
\delta\Upsilon_{\mathrm{i}} &= \delta\Upsilon_{\mathrm{i}}^{\dagger} + \delta\Upsilon_{\mathrm{i}}^{\ddagger} \\
&= \delta\underline{\mathrm{d}}^{\top} \left(\underline{\underline{\mathrm{K}}}_\sigma + \underline{\underline{\mathrm{K}}}_\gamma \right) \underline{\mathrm{d}} \\
&= \delta\underline{\mathrm{d}}^{\top}\, \underline{\underline{\mathrm{K}}}\, \underline{\mathrm{d}}\,. \qquad (93)
\end{aligned}$$

The principle of virtual works states that the external and the internal virtual works are equal for a general virtual displacement $\delta\underline{\mathrm{d}}$, namely

$$\delta\underline{\mathrm{d}}^{\top}\, \underline{\mathrm{G}} = \delta\Upsilon_{\mathrm{e}} = \delta\Upsilon_{\mathrm{i}} = \delta\underline{\mathrm{d}}^{\top}\, \underline{\underline{\mathrm{K}}}\, \underline{\mathrm{d}}\,, \quad \forall\delta\underline{\mathrm{d}}\,, \qquad (94)$$

if and only if the applied external actions $\underline{\mathrm{G}}$ are in equilibrium with the elastic reactions due to the displacements $\underline{\mathrm{d}}$; the following equality thus holds

$$\underline{\mathrm{G}} = \underline{\underline{\mathrm{K}}}\, \underline{\mathrm{d}}\,; \qquad (95)$$

the $\underline{\underline{\mathrm{K}}}$ *stiffness matrix* relates a deformed element configuration, which is defined based on the generalized displacement vector $\underline{\mathrm{d}}$, with the $\underline{\mathrm{G}}$ generalized forces that have to be applied at the element nodes to keep the element in such a stretched state.

0.3.6 The shear locking flaw

Figures 8 rationalize the shear locking phenomenon that plagues the plain bilinear isoparametric element in its mimicking the pure bending deformation modes; the case of an in-plane constant curvature bending is presented, but an analogous behaviour is observed in the out-of-plane bending case.

In Figure 8a, a rectangular[37] planar element is presented, whose geometry is defined by the a/b side length ratio, being the thickness not relevant for the treatise. The material is assumed linearly elastic, homogeneous and isotropic.

In Figure 8b, the exact solution for an equivalent prismatic body subject to pure bending is presented in terms of strain components and strain energy area density, as a function of the imposed angular displacement of the ends. The first Castigliano theorem may be employed in deriving the applied bending moment C_{b}, as predicted by the exact solution.

In Figure 8c, the same angular displacement is imposed to the flanks of a four-noded, isoparametric element of the kind described in the present treatise. The trapezoidal (or *keystoning*) deformation shown in Figure is the best-effort exact solution mimicking we may obtain with a single element.

In the absence of OOP displacements and IP rotations, a pure membrane deformation is obtained; the drilling DOF is not considered. Strain components are derived according to the proposed formulation, and reported along the strain energy area density; apart from the ϵ_x longitudinal strain, inconsistencies are observed with respect to the exact solution. Again, the first Castigliano theorem may be employed in deriving the bending moment C_{iso4}, as predicted by the element formulation.

In Figure 8d, the exact solution is subtracted from its finite element counterpart, thus revealing a spurious residual strain field, whose most notable characteristic is a generally nonzero IP shear strain component γ_{xy}. Such a component is constant in the transverse to bending direction y, whereas it linearly varies in the axial direction x from $+\alpha/2$ to $-\alpha/2$, being null at the $x = 0$ (or $\xi = 0$) locus alone.

Such a spurious shear component contributes to the element strain

[37] vs. generally quadrangular, for the sake of treatise simplicity

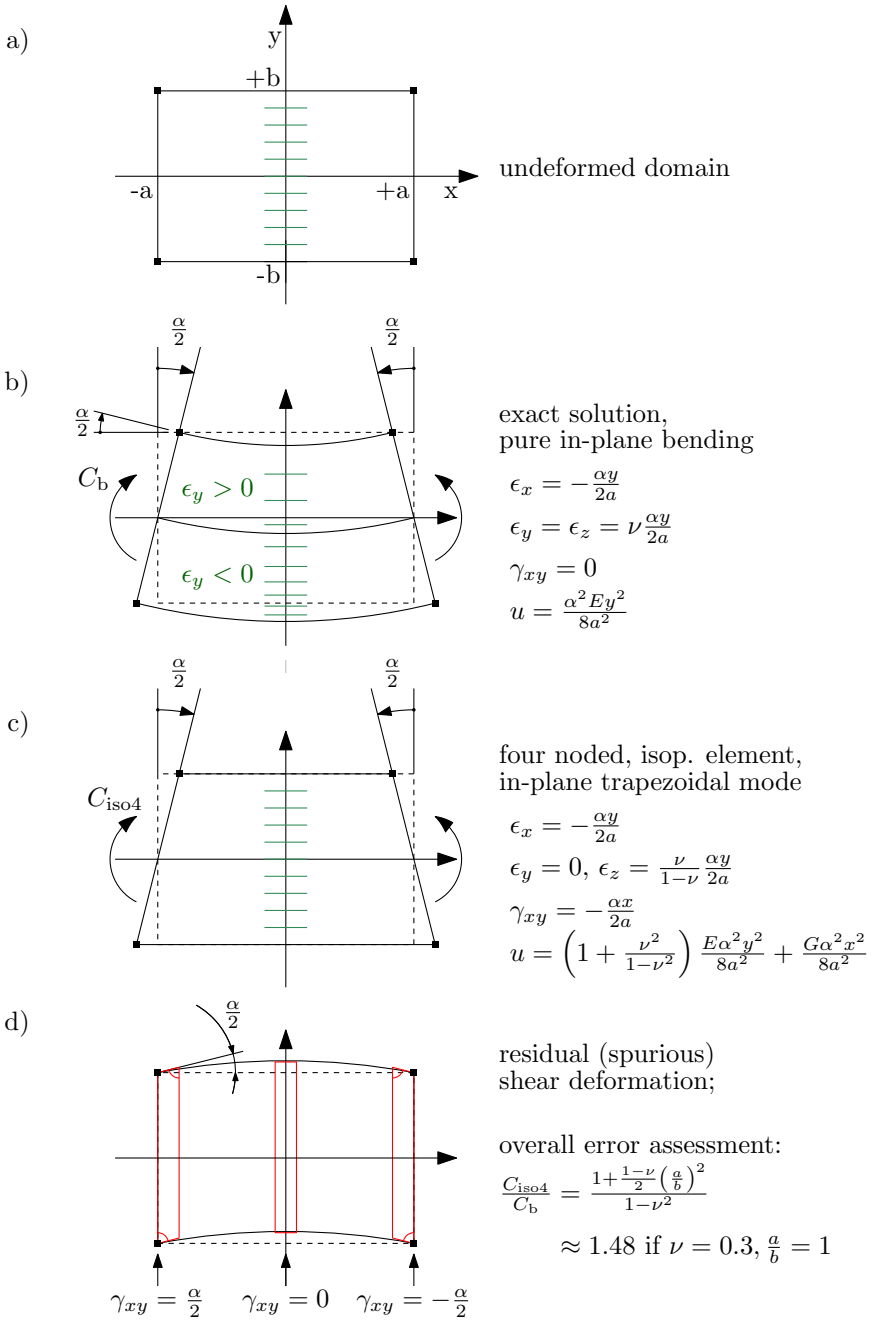

Figure 8: Rationalization of the [IP] shear locking phenomenon, in the case of a rectangular plate element. An analogous construction may be derived for the OOP counterpart.

energy thus stiffening the element with respect to the exact solution; the ratio between the bending moments to be applied to induce a given curvature is also reported, which reveals that a $\approx +48\%$ bogus stiffening is to be expected for the geometrically regular element, and the commonest structural materials.

In particular the error grows with the a/b ratio, and it becomes consistent with that due the sole $\sigma_y = 0$ vs. $\epsilon_y = 0$ incongruity ($\approx +9.8\%$) in the limit case of $a/b \to 0$.

If such a spurious stiffening is tolerable for the in-plane bending – which is a secondary loadcase for a thin walled body, the analogous results obtained in the more significant transverse deflection (out-of-plane) bending case makes the element under scrutiny not compliant with the Irons patch test[38] for plates – i.e., some error due to discretization is noticed even in the uniform curvature bending loadcase.

Many workarounds are proposed in literature, see e.g. the chapters devoted to the topic in [8]; in the following, two emending techniques are presented, which are (apparently[39]) employed for the MSC.Marc Element 75.

A solution for the oop plate bending

An ingenious sampling and interpolation technique has been developed in [9] that overcomes the locking effect due to the spurious transverse shear strain that develops when the element is subject to out-of-plane bending. Such technique, however, does not correct the element behaviour with respect to in-plane bending.

Eqn. 79 is employed in obtaining the tranverse shear strain components $\bar{\gamma}_{zx}$ and $\bar{\gamma}_{yz}$ at the edge midpoints; the edge-aligned component $\bar{\gamma}_{z\widehat{ij}}$ is derived by projection along the $\widehat{ij}$ direction, whereas the orthogonal component is neglected.

Figure 9a evidences that a null spurious tranverse shear is measured at the midpoint of the 12 and of the 41 edges when a constant, out-of-plane curvature is locally enforced that develops along the $\widehat{12}$ and the

[38] in summary: a finite element formulation passes the patch test if an arbitrarily coarse discretization still exactly forecasts any uniform [generalized] strain solution, given a conformable set of boundary conditions; see [6], and [7] for some further developments.

[39] Documentation is not as detailed, and the source code is not available; some literature search and some reverse engineering hints for the usage of such techniques.

$\widehat{41}$ directions, respectively. Such property holds for all edges.

In Figure 9b, a differential out-of-plane displacement is added to the initial pure bending configuration of Fig. 9a, and in the absence of further rotations at nodes; a proper (vs. spurious) transverse shear strain field is thus induced in the element, that the sampling scheme must properly evaluate.

The edge aligned, transverse shear components sampled at the side midpoints are then assigned to the whole edge, and in particular to both its extremal nodes.

As shown in Figure 9b (and in the related enlarged view), two independent transverse shear components $\bar{\gamma}_{z\widehat{12}}$ and $\bar{\gamma}_{z\widehat{41}}$ are associated to the n1 node, which is taken as an example.

A vector is uniquely determined, whose projections on the $\widehat{12}$ and $\widehat{41}$ directions coincide with the associated transverse shear components; the components of such vector with respect to the x, y axes define the $\bar{\gamma}_{zx,\mathrm{n1}}$ and $\bar{\gamma}_{yz,\mathrm{n1}}$ tranverse shear terms at the n1 node.

Such procedure is repeated for all the element vertices; the obtained nodal values for the transverse shear components are then interpolated to the element interior, according to the customary bilinear scheme.

Due to the peculiarity of the initial sampling points, the obtained tranverse shear strain field is amended with respect to the spurious contribution that previously led to the shear locking effect; the usual quadrature scheme may now be employed.

Equation 79 still formalizes the passage from nodal DOFs to the out-of-plane shear field, since the procedure described in the present paragraph may be easily cast in the form of a revised $\underline{\underline{\mathrm{B}}}_\gamma$ matrix.

A solution for the ip plate bending, which also mitigates the drilling mode quirks.

TODO.

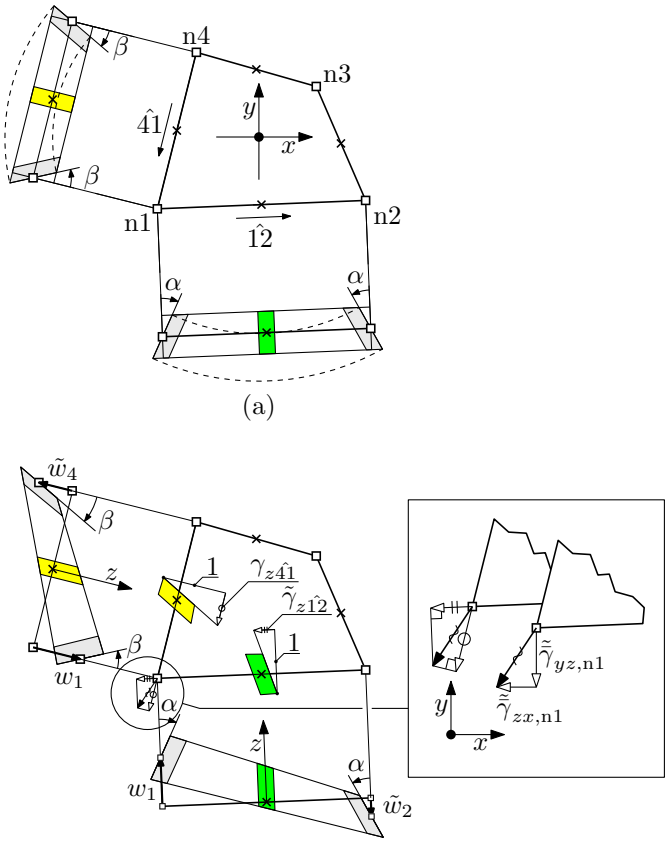

Figure 9: A transverse shear sampling technique employed in the four-noded isoparametric element for preventing shear locking in the OOP plate bending.

0.4 Mass matrix for the finite element

0.4.1 Energy consistent formulation for the mass matrix

The Ω volume of material associated to a finite element is considered, along with the local, physical reference system (x, y, z), and its isoparametric counterpart that, for the quadrilateral plate element under scrutiny, is embodied by the (ξ, η, z) triad.

The *vector* shape function array

$$\underline{\underline{\mathrm{S}}}\,(\xi, \eta, z) = \begin{bmatrix} \dots & \tilde{u}_i(\xi, \eta, z) & \dots \\ \dots & \tilde{v}_i(\xi, \eta, z) & \dots \\ \dots & \tilde{w}_i(\xi, \eta, z) & \dots \end{bmatrix} \tag{96}$$

is defined based on the elementary motions $\underline{\tilde{\mathrm{u}}}_i \equiv [\tilde{u}_i, \tilde{v}_i, \tilde{w}_i]^\top$ induced to the element material points by imposing a unit value to the i-th degree of freedom d_i, while keeping the others fixed.

The displacement field is then defined as a linear combination of the elementary motions above, where the $\underline{\mathrm{d}}$ element DOFs serve as coefficients, namely

$$\underline{\mathrm{u}}\,(\xi, \eta, z) = \underline{\underline{\mathrm{S}}}\,(\xi, \eta, z)\,\underline{\mathrm{d}}\,. \tag{97}$$

Deriving with respect to time the equation above, the velocity field

$$\underline{\dot{\mathrm{u}}}\,(\xi, \eta, z) = \underline{\underline{\mathrm{S}}}\,(\xi, \eta, z)\,\underline{\dot{\mathrm{d}}} \tag{98}$$

is obtained as a function of the first variation in time of element DOFs. Expression 98 is simplified by the constant-in-time nature of $\underline{\underline{\mathrm{S}}}$.

The kinetic energy contribution associated to the deformable element material points may be integrated, thus obtaining

$$E_{\mathrm{kin}} = \frac{1}{2} \iiint_{\Omega} \underline{\dot{\mathrm{u}}}^{\top}\, \underline{\dot{\mathrm{u}}}\, \rho d\Omega \tag{99}$$

where ρ is the material mass density, that may vary across the domain. By substituting the velocity field definition of Eq. 98 we obtain

$$E_{\mathrm{kin}} = \frac{1}{2} \iiint_{\Omega} \left[\underline{\underline{\mathrm{S}}}\,\underline{\dot{\mathrm{d}}}\right]^{\top} \left[\underline{\underline{\mathrm{S}}}\,\underline{\dot{\mathrm{d}}}\right] \rho d\Omega, \tag{100}$$

and finally

$$E_{\text{kin}} = \frac{1}{2}\,\underline{\dot{\mathrm{d}}}^{\top}\left[\iiint_{\Omega}\underline{\underline{\mathrm{S}}}^{\top}\,\underline{\underline{\mathrm{S}}}\,\rho d\Omega\right]\,\underline{\dot{\mathrm{d}}} = \frac{1}{2}\,\underline{\dot{\mathrm{d}}}^{\top}\,\underline{\underline{\mathrm{M}}}\,\underline{\dot{\mathrm{d}}}\,. \tag{101}$$

The integral term that defines the $\underline{\underline{\mathrm{M}}}$ *mass* matrix is evaluated by resorting to the same quadrature technique introduced for its stiffness counterpart.

The actual nature of the mass matrix terms varies based on the type of the DOFs that are associated to the term row and column; in particular, the diagonal terms that are related to displacements and rotations are dimensionally consistent with a mass and a moment of inertia, respectively.

The mass matrix quantifies the inertial response of the finite element; according to its definition

$$\underline{\underline{\mathrm{M}}} = \iiint_{\Omega}\underline{\underline{\mathrm{S}}}^{\top}\,\underline{\underline{\mathrm{S}}}\,\rho d\Omega, \tag{102}$$

it is merely a function of the material density, and of the kinematic laws that constrain the motion of the material particles within the element.

If a set of external (generalized) forces $\underline{\mathrm{G}}$ is applied to the element DOFs in the fictitious absence of elastic reactions, a purely inertial response is expected. The $\underline{\dot{\mathrm{d}}}$ vector defines the instantaneous first derivative in time of the DOFs (i.e. nodal translational and rotational velocities); the instantaneous power supplied by the external forces is then evaluated as $\underline{\dot{\mathrm{d}}}^{\top}\,\underline{\mathrm{G}}$, that induces an equal time derivative of the kinetic energy, quantified as [40]

$$\begin{aligned}\underline{\dot{\mathrm{d}}}^{\top}\,\underline{\mathrm{G}} = \frac{dE_{\text{kin}}}{dt} =& \frac{d}{dt}\left(\frac{1}{2}\,\underline{\dot{\mathrm{d}}}^{\top}\,\underline{\underline{\mathrm{M}}}\,\underline{\dot{\mathrm{d}}}\right)\\ =& \frac{1}{2}\left(\underline{\ddot{\mathrm{d}}}^{\top}\,\underline{\underline{\mathrm{M}}}\,\underline{\dot{\mathrm{d}}} + \underline{\dot{\mathrm{d}}}^{\top}\,\underline{\underline{\mathrm{M}}}\,\underline{\ddot{\mathrm{d}}}\right)\\ =& \underline{\dot{\mathrm{d}}}^{\top}\,\underline{\underline{\mathrm{M}}}\,\underline{\ddot{\mathrm{d}}}\,.\end{aligned}$$

[40] The symmetric matrix characterizing property

$$\underline{\mathrm{x}}^{\top}\,\underline{\underline{\mathrm{A}}}\,\underline{\mathrm{y}} = \underline{\mathrm{y}}^{\top}\,\underline{\underline{\mathrm{A}}}\,\underline{\mathrm{x}} \quad \forall\underline{\mathrm{x}},\underline{\mathrm{y}} \in \mathbb{R}^{n}$$

is used in deriving the last passage.

Due to the general nature of $\underline{\dot{d}}$, equality

$$\underline{G} = \underline{\underline{M}}\, \underline{\ddot{d}} \tag{103}$$

is implied, which points out the mass matrix role in transforming the DOF vector second derivative in time (i.e. nodal translational and rotational accelerations) into the generalized force components that are to be applied in order to sustain such variation of motion.

0.4.2 Lumped mass matrix formulation

In a few applications, a diagonal form for the mass matrix is preferred at the expense of a) a strict adherence to energy consistency with regard to rotational motions, and b) some arbitrariness in its definition.

The finite element volume is ideally partitioned into a set of influence domains, one each node. In the case of the four-noded quadrilateral, material points whose ξ, η isoparametric coordinates fall within the first, second, third and fourth quadrant are associated to nodes n3, n4, n1 and n2, respectively; those distributed masses are then ideally accumulated at the associated node.

A group of four concentrated nodal masses is thus defined, whose motion is defined based on single translational DOFs, and not on the plurality of weighted contributions that induces the nonzero, nondiagonal terms at the consistent mass matrix.

This undue material accumulation at the element periphery produces a spurious increase of the moment of inertia, condition, this, that may only be worsened if (positive) rotational inertias are introduced at nodes.

Those nodal rotational inertias are however required in associating a bounded angular acceleration to unbalanced nodal torques; solution methods based on the mass matrix inversion, e.g. explicit dynamic procedures, are precluded otherwise. Since there is no consensus on the quantification those inertial terms, the reader is addressed to specialized literature.

The effect of this elemental overestimation on the rotational inertia of the modeled structures decreases with mesh refinement, and it vanishes for a theoretically vanishing element size.

0.5 External forces

Energetically consistent external actions may be applied at the nodal DOFs, that may be interpreted as *concentrated* forces and moments; their physical rationalization outside the discretized structure framework – and in particular back to the underlying elastic continua theory – is far from being trivial.

Surface tractions and volumetric loads are instead naturally tied with the continuum formulation, and are usually employed in formalizing the load condition of structural components.

The present paragraph derives the equivalent nodal representation of distributed actions acting on the domain of a single finite element; the inverse relation provides a finite, distributed traction counterpart to concentrated actions applied at the nodes of a discretized FE model.

The $\underline{\underline{\mathrm{S}}}$ set of elementary deformation modes that is introduced in the context of the element mass matrix derivation, see Eqn. 96, is employed to define a virtual displacement field within the element domain based on the virtual variation $\delta\,\underline{\mathrm{d}}$ of its nodal DOFs values, i.e.

$$\delta\,\underline{\mathrm{u}}\,(\xi,\eta,z) = \underline{\underline{\mathrm{S}}}\,(\xi,\eta,z)\delta\,\underline{\mathrm{d}}\,, \tag{104}$$

see also Eq. 97.

A volumetric external load is considered, whose components $\underline{\mathrm{p}} = [p_x, p_y, p_z]$ are consistent with the $\underline{\underline{\mathrm{S}}}$ matrix reference system, i.e. the local to the element, physical Cxyz one. If external load components are defined in the context of a global reference system, straightforward reference frame transformations are to be applied.

The virtual work performed by those distributed actions is first integrated along the element domain, and then equalled to its nodal counterpart $\delta\,\underline{\mathrm{d}}^{\top}\,\underline{\mathrm{F}}$, thus leading to

$$\begin{aligned}
\delta\,\underline{\mathrm{d}}^{\top}\,\underline{\mathrm{F}} &= \iiint_{\Omega} (\delta\,\underline{\mathrm{u}})^{\top}\;\underline{\mathrm{p}}\,d\Omega \\
&= \iiint_{\Omega} \left(\underline{\underline{\mathrm{S}}}\,\delta\,\underline{\mathrm{d}}\right)^{\top}\;\underline{\mathrm{p}}\,d\Omega \\
&= \delta\,\underline{\mathrm{d}}^{\top} \iiint_{\Omega} \underline{\underline{\mathrm{S}}}^{\top}\,\underline{\mathrm{p}}\,d\Omega,
\end{aligned}$$

and finally to

$$\underline{\mathrm{F}} = \iiint_{\Omega} \underline{\underline{\mathrm{S}}}^{\top}\,\underline{\mathrm{p}}\,d\Omega \tag{105}$$

due to the general nature of $\delta \underline{\mathrm{d}}$.

In the case of the plate element under scrutiny, we recall that the volume integral of Eq. 105 is numerically evaluated according to Eq. 91 quadrature scheme.

In general, the quadrature along the domain is performed according to the methods introduced for deriving the element stiffness matrix. If a surface or an edge load are supplied in place of the volumetric load vector $\underline{\mathrm{p}}$, Eq. 105 integral may be adapted to span each loaded element face, or edge.

In the case of low order isoparametric elements – e.g. the four-noded quadrilateral shell element, an alternative, simplified procedure for the consolidation of the distributed loads into nodal forces becomes viable. According to such procedure, the element domain is partitioned into influence volumes, one each node; the external load contributions are then accumulated within each partition, and the resultant force vector is applied to the associated node.

By moving such resultant force from the distribution center of gravity (COG) to the corner node, momentum balance is naively disregarded; the induced error however decreases with the load field variance across the element, and hence with the element size. Such error vanishes for uniform distributed loads.

In the presence of a better established, work consistent counterpart, such simplified procedure is mostly employed to set a rule-of-thumb equivalence between distributed and nodal loads; in particular, the stress-singular nature of a set of nodal loads may be easily pointed out if it is observed that a finite load resultant is applied to influence areas that cumulatively vanish with vanishing element size.

0.6 Joining elements into structures.

0.6.1 Displacement and rotation field continuity

Displacement and rotation fields are continuous at the isoparametric quadrilateral inter-element interfaces; they are in fact continuous at nodes since the associated nodal DOFs are shared by adjacent elements, and the field interpolations that occur within each quadrilateral domain a) they both reduce to the same linear relation along the shared edge, and b) they are performed in the absence of any contributions related to unshared nodes or DOFs.

A similar result does not hold for the [generalized] strain and stress components, which are in general discontinuous across the element boundaries; such a discontinuity – which vanishes with mesh refinement except at singularities[41] – constitutes an indicator of the FE discretization error.

0.6.2 Expressing the element stiffness matrix in terms of global dofs

As seen in Par. 0.3.5, the stiffness matrix of each j-th element defines the elastic relation between the associated generalized forces and displacements, i.e.

$$\underline{\mathrm{G}}_{\mathrm{e}j} = \underline{\underline{\mathrm{K}}}_{\mathrm{e}j}\, \underline{\mathrm{d}}_{\mathrm{e}j} \tag{106}$$

where the DOFs definition is local with respect to the element under scrutiny.

In order to investigate the mutual interaction between elements in a structure, a common set of *global* DOFs is required; in particular, generalized displacement DOFs are defined at each l-th global node, i.e., for nodes interacting with the shell element formulation under scrutiny,

$$\underline{\mathrm{d}}_{\mathrm{g}l} = \begin{bmatrix} u_{\mathrm{g}l} \\ v_{\mathrm{g}l} \\ w_{\mathrm{g}l} \\ \theta_{\mathrm{g}l} \\ \varphi_{\mathrm{g}l} \\ \psi_{\mathrm{g}l} \end{bmatrix} . \tag{107}$$

[41] i.e. at locations at which a singularity (or a discontinuity) of the *exact* solution may be theoretically predicted

The global reference system $OXYZ$ is typically employed in projecting nodal vector components. However, each l-th global node may be supplied with a specific reference system, whose unit vectors are $\hat{\imath}_{gl}, \hat{\jmath}_{gl}, \hat{k}_{gl}$, thus permitting the employment of non uniformly aligned (e.g. cylindrical) global reference systems.

Those nodal degrees of freedom may be collected in a global DOFs vector

$$\underline{\mathrm{d}}_{\mathrm{g}}^{\top} = \begin{bmatrix} \underline{\mathrm{d}}_{\mathrm{g1}}^{\top} & \underline{\mathrm{d}}_{\mathrm{g2}}^{\top} & \dots & \underline{\mathrm{d}}_{\mathrm{g}l}^{\top} & \dots & \underline{\mathrm{d}}_{\mathrm{g}n}^{\top} \end{bmatrix} \tag{108}$$

that parametrically defines any deformed configuration of the structure.

Analogously, a global, external (generalized[42]) forces vector may be defined, that assumes the form

$$\underline{\mathrm{F}}_{\mathrm{g}}^{\top} = \begin{bmatrix} \underline{\mathrm{F}}_{\mathrm{g1}}^{\top} & \underline{\mathrm{F}}_{\mathrm{g2}}^{\top} & \dots & \underline{\mathrm{F}}_{\mathrm{g}l}^{\top} & \dots & \underline{\mathrm{F}}_{\mathrm{g}n}^{\top} \end{bmatrix}; \tag{109}$$

since single DOF (or single-DOF(!) constraint (SPC)) and multi DOF (or multi-DOF(!) constraint (MPC)) kinematic constraints[43] are expected to be applied to the structure DOFs, the following vector of reaction forces

$$\underline{\mathrm{R}}_{\mathrm{g}}^{\top} = \begin{bmatrix} \underline{\mathrm{R}}_{\mathrm{g1}}^{\top} & \underline{\mathrm{R}}_{\mathrm{g2}}^{\top} & \dots & \underline{\mathrm{R}}_{\mathrm{g}l}^{\top} & \dots & \underline{\mathrm{R}}_{\mathrm{g}n}^{\top} \end{bmatrix} \tag{110}$$

is introduced. Many FE softwares – and MSC.Marc in particular – treat external and internal constraints separately, thus leading to two set of constraint actions, namely the (strictly named) *reaction forces*, and the *tying forces*, respectively; for the sake of simplicity, the constraint treatise is unified in the present contribution.

The simple four element, roof-like structure of Fig. 10 is employed in the following to discuss the procedure that derives the elastic response characterization for the structure from its elemental counterparts.

The structure comprises nine nodes, whose location in space is defined according to a global reference system $OXYZ$, see Table 2.

[42] Unless otherwise specified, the *displacement* and *force* terms refer to the DOFs, and the suitable actions that perform work with their variation, respectively. They are in fact *generalized* forces and displacements.

[43] in a previous version of this contribution, an equivalency was proposed between the single DOF vs. multi DOF constraint characterization, and the *external* – i.e. *to ground* – vs. *internal* classification. In fact, those classifications are disjoint, since, if ground reactions are expected in the single DOF case, legitimate multi DOF constraint exist – e.g. the hypothetical $u_{g2} = v_{g5}$ – whose reactions are not self-equilibrated, and hence require an external, ground intervention for their balancing.

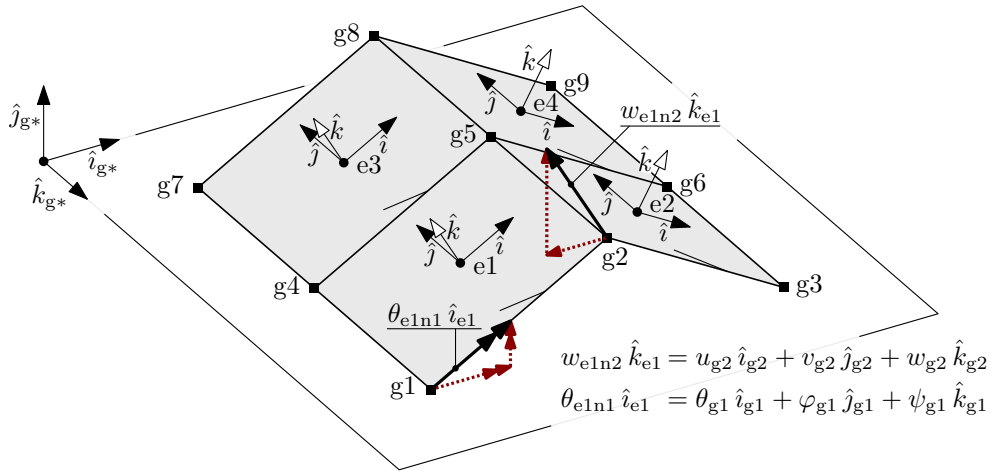

Figure 10: A simple four-element, roof-like structure employed in discussing the assembly procedures. The elements are square, thick plates whose angle with respect to the global XY plane is 30°

node	X	Y	Z
g1	$-lc$	0	$+l$
g2	0	$+ls$	$+l$
g3	$+lc$	0	$+l$
g4	$-lc$	0	0
g5	0	$+ls$	0
g6	$+lc$	0	0
g7	$-lc$	0	$-l$
g8	0	$+ls$	$-l$
g9	$+lc$	0	$-l$

Table 2: Nodal coordinates for the roof-like structure of Figure 10. l is the element side length, $c = \cos 30°$ and $s = \sin 30°$

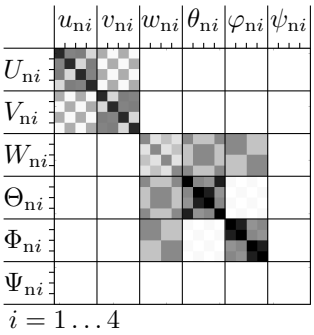

Figure 11: A representation of the stiffness matrix terms for each element in the example structure; the term magnitude is represented through a linear grayscale, spanning from zero (white) to the peak value (black).

	n1	n2	n3	n4
e1	g1	g2	g5	g4
e2	g2	g3	g6	g5
e3	g4	g5	g8	g7
e4	g5	g6	g9	g8

Table 3: Element connectivity for the roof-like structure of Figure 10. As an example, the node described by the local numbering e3n2 is mapped to the global node g5.

The structure is composed by four, identical, four noded isoparametric shell elements, whose formulation is described in the preceding section 0.3.

A grayscale, normalized representation of the element stiffness matrix is shown in Figure 11, where the white to black colormap spans from zero to the maximum in absolute value term.

The mapping between local, element based node numbering and the global node numbering is reported in the connectivity Table 3.

Such i) local to global node numbering mapping, together with ii) the change in reference system mentioned above, defines a set of elemental DOF mapping matrices, $\underline{\underline{\mathrm{P}}}_{ej}$, one each j-th element. Such matrices are defined as follows: the i-th row the $\underline{\underline{\mathrm{P}}}_{ej}$ matrix contains the coefficients of the linear combination of global DOFs that equates

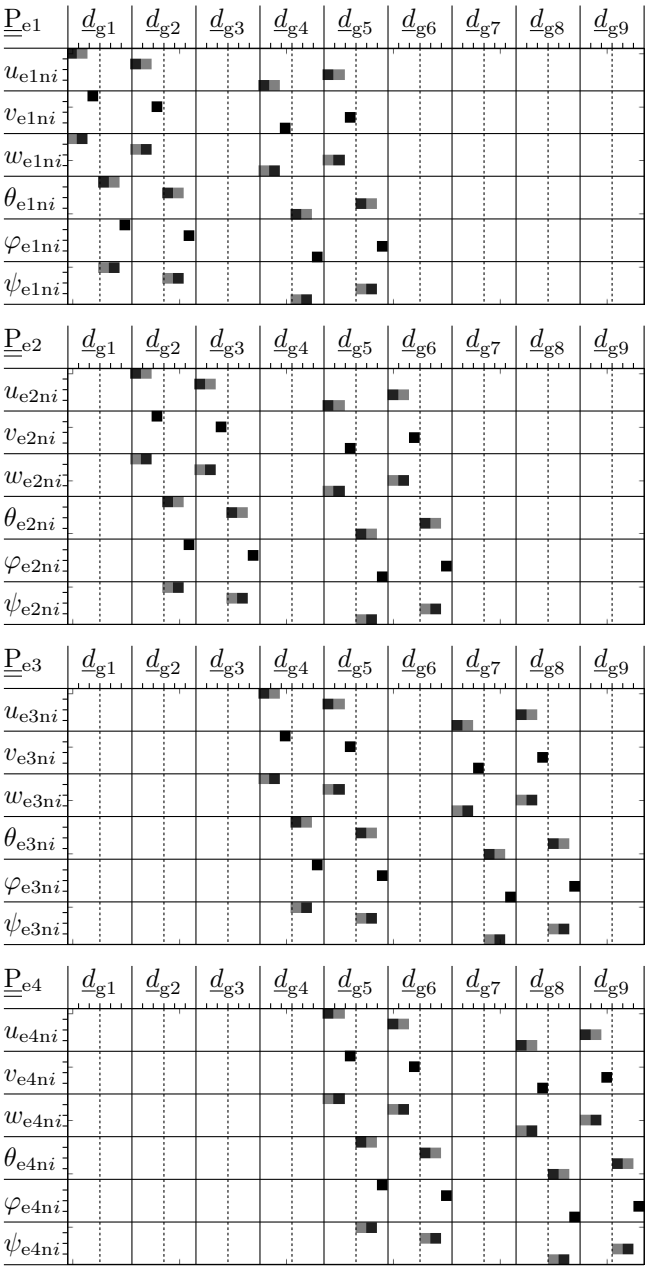

Figure 12: A grayscale representation of the terms of the four $\underline{\underline{\mathrm{P}}}_{\mathrm{e}j}$ mapping matrices associated the elements of Fig. 10. The colormap spans from white (zero) to black (one); the lighter and the darker grey colors represent terms that equate in modulus $\sin 30°$ and $\cos 30°$, respectively.

the i local DOF of the j-th element; an example is proposed in the following to illustrate such relation.

With reference to the structure of Figure 10, w_{e1n2} and θ_{e1n1} respectively represent the 10th and the 13th local degrees of freedom of element 1.

Their global representation involves a subset of the g2 and g1 global nodes DOFs, respectively, namely

$$w_{\mathrm{e1n2}} = \langle \hat{k}_{\mathrm{e1}}, \hat{\imath}_{\mathrm{g2}} \rangle u_{\mathrm{g2}} + \langle \hat{k}_{\mathrm{e1}}, \hat{\jmath}_{\mathrm{g2}} \rangle v_{\mathrm{g2}} + \langle \hat{k}_{\mathrm{e1}}, \hat{k}_{\mathrm{g2}} \rangle w_{\mathrm{g2}} \tag{111}$$

$$\theta_{\mathrm{e1n1}} = \langle \hat{\imath}_{\mathrm{e1}}, \hat{\imath}_{\mathrm{g1}} \rangle \theta_{\mathrm{g1}} + \langle \hat{\imath}_{\mathrm{e1}}, \hat{\jmath}_{\mathrm{g1}} \rangle \phi_{\mathrm{g1}} + \langle \hat{\imath}_{\mathrm{e1}}, \hat{k}_{\mathrm{g1}} \rangle \psi_{\mathrm{g1}} \tag{112}$$

where $\hat{\imath}_{\mathrm{e1}}$,$\hat{\jmath}_{\mathrm{e1}}$, $\hat{k}_{\mathrm{e1}}$ are the orientation vectors of the element 1 local reference system, $\hat{\imath}_{\mathrm{g1}}$,$\hat{\jmath}_{\mathrm{g1}}$,$\hat{k}_{\mathrm{g1}}$ and $\hat{\imath}_{\mathrm{g2}}$,$\hat{\jmath}_{\mathrm{g2}}$,$\hat{k}_{\mathrm{g2}}$ are the orientation vectors of the global nodes 1 and 2 reference systems, and $\langle \cdot, \cdot \rangle$ represents their mutual scalar product, or, equivalently, the cosinus of the angle between two unit vectors.

The 10th and the 13th row of the $\underline{\underline{\mathrm{P}}}_{\mathrm{e1}}$ mapping matrix are defined based on Eqs.111 and 112, respectively, and they are null except for the elements

$$\left[\underline{\underline{\mathrm{P}}}_{\mathrm{e1}}\right]_{10,7} = \langle \hat{k}_{\mathrm{e1}}, \hat{\imath}_{\mathrm{g2}} \rangle \qquad \left[\underline{\underline{\mathrm{P}}}_{\mathrm{e1}}\right]_{13,4} = \langle \hat{\imath}_{\mathrm{e1}}, \hat{\imath}_{\mathrm{g1}} \rangle$$

$$\left[\underline{\underline{\mathrm{P}}}_{\mathrm{e1}}\right]_{10,8} = \langle \hat{k}_{\mathrm{e1}}, \hat{\jmath}_{\mathrm{g2}} \rangle \qquad \left[\underline{\underline{\mathrm{P}}}_{\mathrm{e1}}\right]_{13,5} = \langle \hat{\imath}_{\mathrm{e1}}, \hat{\jmath}_{\mathrm{g1}} \rangle$$

$$\left[\underline{\underline{\mathrm{P}}}_{\mathrm{e1}}\right]_{10,9} = \langle \hat{k}_{\mathrm{e1}}, \hat{k}_{\mathrm{g2}} \rangle \qquad \left[\underline{\underline{\mathrm{P}}}_{\mathrm{e1}}\right]_{13,6} = \langle \hat{\imath}_{\mathrm{e1}}, \hat{k}_{\mathrm{g1}} \rangle,$$

being u_{g2},v_{g2},w_{g2},θ_{g1},ϕ_{g1} and ψ_{g1} the 7th, 8th, 9th, 4th, 5th and 6th global degrees of freedom according to their position in $\underline{\mathrm{d}}_{\mathrm{g}}$.

Figure 12 presents a grayscale representation of the four $\underline{\underline{\mathrm{P}}}_{\mathrm{e}j}$ matrices; please note the extremely sparse nature of those matrices, whose number of nonzero terms scales with the single element DOF cardinality, whereas the total number of terms scale with the whole structure DOF cardinality.

The rows of the rectangular $\underline{\underline{\mathrm{P}}}_{\mathrm{e}j}$ mapping matrix are mutually orthonormal; the mapping matrix is orthogonal in the sense of the Moore-Penrose pseudoinverse, since its transpose and its pseudoinverse coincide.

By resorting to the elemental DOF mapping matrix artifice, the j-th element DOFs may be derived from their global counterpart as

$$\underline{\mathrm{d}}_{\mathrm{e}j} = \underline{\underline{\mathrm{P}}}_{\mathrm{e}j}\, \underline{\mathrm{d}}_{\mathrm{g}}, \quad \forall j. \tag{113}$$

Eq. 106 let us further derive the component of external actions that are required by each j-th stretched element to oppose the its own elastic reactions as

$$\underline{\mathrm{G}}_{\mathrm{e}j} = \underline{\underline{\mathrm{K}}}_{\mathrm{e}j}\, \underline{\underline{\mathrm{P}}}_{\mathrm{e}j}\, \underline{\mathrm{d}}_{\mathrm{g}}, \quad \forall j; \tag{114}$$

such a external action vector, which is still expressed in terms of the local set of DOFs, is now formulated as a function of the global displacement vector. Those elemental external action components $\underline{\mathrm{G}}_{\mathrm{e}j}$ may be cast in terms of the global DOF set based on the following virtual work equivalency

$$\delta\underline{\mathrm{d}}_{\mathrm{g}}^{\top}\, \underline{\mathrm{G}}_{\mathrm{g}\leftarrow\mathrm{e}j} = \left(\underline{\underline{\mathrm{P}}}_{\mathrm{e}j}\delta\underline{\mathrm{d}}_{\mathrm{g}}\right)^{\top}\, \underline{\mathrm{G}}_{\mathrm{e}j}, \quad \forall\, \delta\underline{\mathrm{d}}_{\mathrm{g}} \tag{115}$$

where $\underline{\mathrm{d}}_{\mathrm{g}}$ is a generic global virtual displacement, $\underline{\underline{\mathrm{P}}}_{\mathrm{e}j}\delta\underline{\mathrm{d}}_{\mathrm{g}}$ is the associated virtual variation of the j-th element DOFs, see Eq.113, and

$$\underline{\mathrm{G}}_{\mathrm{g}\leftarrow\mathrm{e}j} = \underline{\underline{\mathrm{P}}}_{\mathrm{e}j}^{\top}\, \underline{\mathrm{G}}_{\mathrm{e}j} \tag{116}$$

is the global counterpart of the local $\underline{\mathrm{G}}_{\mathrm{e}j}$ nodal action vector.

Based on 106, 113 and 116, the contribution of the j-th element to the elastic response of the structure may finally be described as the vector of global force components

$$\underline{\mathrm{G}}_{\mathrm{g}\leftarrow\mathrm{e}j} = \underline{\underline{\mathrm{P}}}_{\mathrm{e}j}^{\top}\, \underline{\underline{\mathrm{K}}}_{\mathrm{e}j}\, \underline{\underline{\mathrm{P}}}_{\mathrm{e}j}\, \underline{\mathrm{d}}_{\mathrm{g}}; \tag{117}$$

that have to be applied at the structure DOFs in order to equilibrate the elastic reactions that arise at the nodes of the j-th element, if a deformed configuration is prescribed for the latter according to the $\underline{\mathrm{d}}_{\mathrm{g}}$ global displacement mode.

By accumulating the contribution of the various elements in a structure, the overall relation is obtained

$$\underline{\mathrm{G}}_{\mathrm{g}} = \sum_{j} \underline{\mathrm{G}}_{\mathrm{g}\leftarrow\mathrm{e}j} = \left(\sum_{j} \underbrace{\underline{\underline{\mathrm{P}}}_{\mathrm{e}j}^{\top}\, \underline{\underline{\mathrm{K}}}_{\mathrm{e}j}\, \underline{\underline{\mathrm{P}}}_{\mathrm{e}j}}_{\underline{\underline{\mathrm{K}}}_{\mathrm{g}\leftarrow\mathrm{e}j}} \right) \underline{\mathrm{d}}_{\mathrm{g}} = \underline{\underline{\mathrm{K}}}_{\mathrm{g}}\, \underline{\mathrm{d}}_{\mathrm{g}}, \tag{118}$$

that defines the $\underline{\underline{\mathrm{K}}}_{\mathrm{g}}$ global stiffness matrix as an assembly of the $\underline{\underline{\mathrm{K}}}_{\mathrm{g}\leftarrow\mathrm{e}j}$ elemental contributions. The contribute accumulation at each summatory step is graphically represented in Fig. 13, in the case of the example structure of Fig. 10.

The global stiffness matrix is symmetric, and it shows nonzero terms at cells whose row and column indices are associate to two DOFs that are bridged by a direct elastic link – i.e., an element exists, that insists on both the nodes those DOFs pertain; since only a limited number of elements insist on each given node, the matrix is sparse, as shown in Fig. 13d.

An favourable numbering of the global nodes may be searched for, such that the nonzero terms are clustered within a (possibly) narrow band around the diagonal; the resulting stiffness matrix is hence *banded*, condition this that reduces both the storage memory requirements, and the computational effort in applying the various algebraic operators to the matrix.

The stiffness matrix (half-)bandwidth may be predicted by evaluating the bandwidth required for storing each element contribution

$$b_{\mathrm{e}j} = (i_{\max} - i_{\min} + 1)\, l, \tag{119}$$

and retaining the

$$b = \max_{\mathrm{e}j} b_{\mathrm{e}j} \tag{120}$$

peak value; in the formula 119, l is the number of DOF per element node, whereas $i_{\max}$ and $i_{\max}$ are the extremal integer labels associated to the element nodes, according to the global numbering.

0.6.3 External forces assembly

The element vector forces are accumulated to derive global external forces vector $\underline{\mathrm{F}}_{\mathrm{g}}$, as in

$$\underline{\mathrm{F}}_{\mathrm{g}} = \sum_{j} \underline{\underline{\mathrm{P}}}^{\top}_{\mathrm{e}j}\, \underline{\mathrm{F}}_{\mathrm{e}j}; \tag{121}$$

the transposed $\underline{\underline{\mathrm{P}}}^{\top}_{\mathrm{e}j}$ mapping matrix is employed to translate the actions on the local DOFs to their global counterpart.

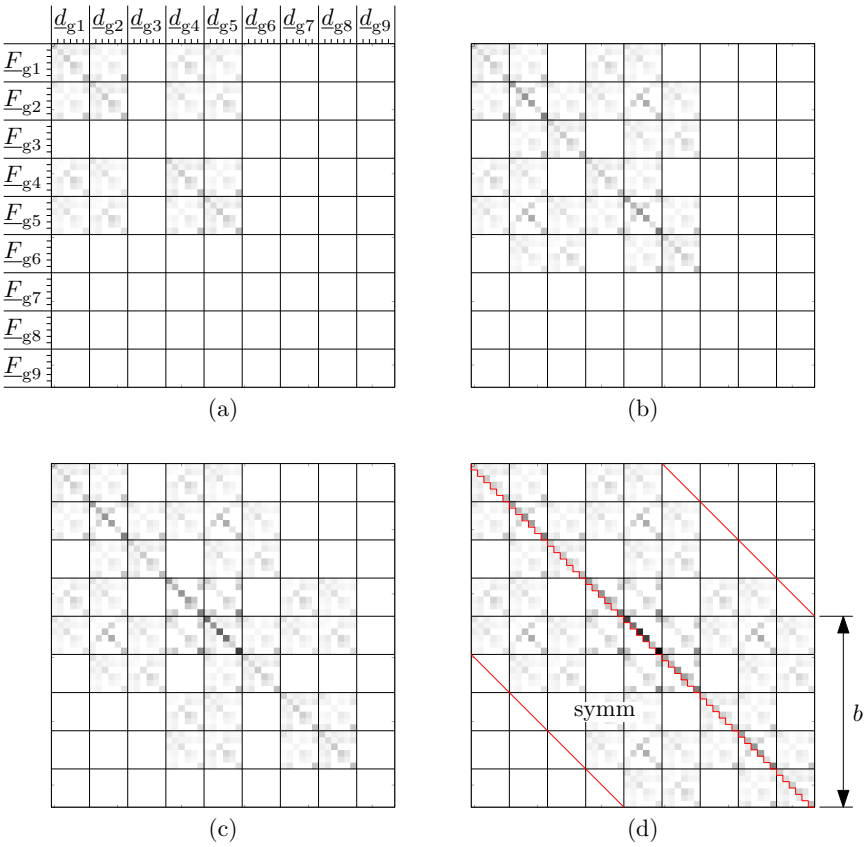

Figure 13: Graphical representation of the assembly steps for the stiffness matrix of the Fig. 10 structure. In (a), the $\underline{\underline{\mathrm{K}}}_{\mathrm{g}\leftarrow\mathrm{e}1}$ term is presented alone; the $\underline{\underline{\mathrm{K}}}_{\mathrm{g}\leftarrow\mathrm{e}2}$, $\underline{\underline{\mathrm{K}}}_{\mathrm{g}\leftarrow\mathrm{e}3}$ and $\underline{\underline{\mathrm{K}}}_{\mathrm{g}\leftarrow\mathrm{e}4}$ are sequentially accumulated, thus leading to (b), (c) and (d). In (d), the symmetric and banded nature of the matrix is evidenced. The zero-initialized form for the matrix that precedes the (a) step is omitted.

0.7 Constraints.

0.7.1 A pedagogical example.

Figure 14 represents a simple, pedagogical example of a three d.o.f. elastic system subject to a set of two kinematic constraints. The first, I, embodies a typical multi d.o.f. constraint[44], namely a 3:1 leverage between the vertical displacements d_3 and d_1 The second, II, consists in a single d.o.f., inhomogeneous constraint that imposes a fixed value to the d_2 vertical displacement.

Both the kinematic constraint may be cast in the same algebraic form

$$\sum_i \alpha_{ji}\, \underline{\mathrm{d}}_i = \underline{\alpha}_j^{\top}\, \underline{\mathrm{d}} = \Delta_j \tag{122}$$

where $j = I, II$ and $i = 1 \dots 3$ the indexes span through the constraints and the model d.o.f.s, respectively, and the $\underline{\alpha}_j$ equation coefficient vectors and inhomogeneous terms are

$$\underline{\alpha}_{\mathrm{I}}^{\top} = \begin{bmatrix} 3 & 0 & 1 \end{bmatrix} \qquad \Delta_{\mathrm{I}} = 0$$
$$\underline{\alpha}_{\mathrm{II}}^{\top} = \begin{bmatrix} 0 & 1 & 0 \end{bmatrix} \qquad \Delta_{\mathrm{II}} = 0.2$$

In the absence of constraints, viable system configurations span the whole $\mathbb{R}^3$ space of Fig. 15 (a); viable configurations with respect to the first constraint alone span the *hyper*-plane/subspace[45] I, whereas the subspace II collects the feasible configurations with respect to the second constraint.

It is relevant to underline that the feasible configuration hyperplanes I and II are normal to the associated coefficient vectors $\underline{\alpha}_{\mathrm{I}}$ and $\underline{\alpha}_{\mathrm{II}}$, respectively.

The $\mathrm{I} \cap \mathrm{II}$ intersection subspace collects the configurations that satisfies both the constraints; such subspace is orthogonal to both $\underline{\alpha}_{\mathrm{I}}$ and $\underline{\alpha}_{\mathrm{II}}$.

If the constraints are assumed as ideal[46], the exerted reactions are orthogonal to the allowed displacements; reaction forces are confined on

[44] usually, and rather improperly, named *multipoint* constraint (MPC)

[45] The subspace of the feasible configurations with respect to a single, scalar linear equation is an hyperplane in the configuration space; due to the limited d.o.f. set cardinality, Figure 15 (a) represents a 2d plane within a 3d space. The *hyper*-nomenclature is preserved to

[46] or, namely, frictionless

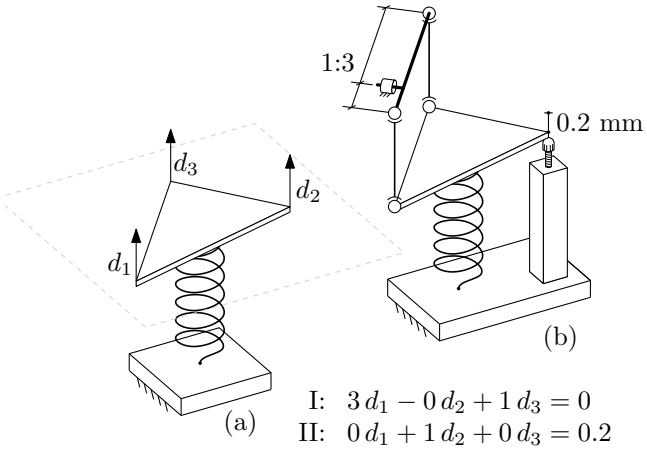

Figure 14: A pedagogical elastic three d.o.f. system, (a), subject to a few kinematic constraints (b).

a subspace of the reaction space that corresponds to[47] the orthogonal complement of the feasible subspace of the configuration space.

By moving on the constraint reaction space shown in 15 (b), the reaction forces associated to constraint I and II are thus proportional to the $\underline{\alpha}_{\mathrm{I}}$ and $\underline{\alpha}_{\mathrm{II}}$ vectors, respectively; the cumulative constraint reactions lie on the linear span of those two vectors, namely span $(\underline{\alpha}_{\mathrm{I}}, \underline{\alpha}_{\mathrm{II}})$.

With reference to some concepts anticipated from the next paragraph, we may set d_1 as the only retained[48] DOF, thus leading to $\underline{\underline{\Lambda}}$ and $\underline{\Delta}$ terms equal to, respectively,

$$\underline{\underline{\Lambda}} = \begin{bmatrix} 1 \\ 0 \\ -3 \end{bmatrix} \qquad\qquad \underline{\Delta} = \begin{bmatrix} 0 \\ 0.2 \\ 0 \end{bmatrix}.,$$

whereas, according to the notation introduced to discuss the Lagrangian

[47] i.e. the two subspaces share, with adjusted physical dimensions, the same generator vectors.

[48] alternatively, d_3 may be chosen for such a role.

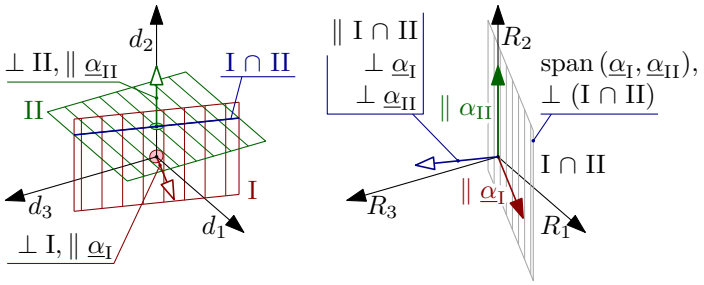

(a) configuration space (b) reaction space

Figure 15: Allowed system configurations and constraint reactions for the pedagogical example of Fig. 14. The allowed displacement sets are easily derived as the homogenous counterpart of (a), and are not represented here.

multiplier formulation, we have

$$\underline{\underline{\mathrm{E}}}_{\mathrm{R}} = \begin{bmatrix} 1 & 0 & 0 \end{bmatrix} \qquad \underline{\underline{\Lambda}}_{\mathrm{TR}} = \begin{bmatrix} 0 \\ -3 \end{bmatrix}$$

$$\underline{\underline{\mathrm{E}}}_{\mathrm{T}} = \begin{bmatrix} 0 & 1 & 0 \\ 0 & 0 & 1 \end{bmatrix} \qquad \underline{\underline{\mathcal{L}}} = \begin{bmatrix} \underline{\alpha}_{\mathrm{II}} & \underline{\alpha}_{\mathrm{I}} \end{bmatrix} \qquad \underline{\Delta}_{\mathrm{T}} = \begin{bmatrix} \Delta_{\mathrm{II}} \\ \Delta_{\mathrm{I}} \end{bmatrix}.$$

0.7.2 General formulation

A set of m constraints

$$d_j = \sum_{d_i \in \underline{\mathrm{d}}_{\mathrm{R}}} \lambda_{ji} d_i + \Delta_j \tag{123}$$

is defined that states the linear[49] dependence of a partition subset of the $\underline{\mathrm{d}}$ DOFs, the d_j *tied* ones, on the remaining d_i terms, that retain their independent nature. The independent terms are collected within a $n - m$ reduced cardinality DOF vector $\underline{\mathrm{d}}_{\mathrm{R}}$, and they are referred to as the *retained* ones[50]. Similarly, the m tied DOF are collected in the $\underline{\mathrm{d}}_{\mathrm{T}}$ vector.

[49] more precisely, *linear variation* dependence, due to the presence of the inhomogeneous term.

[50] Here, the definition of the overall, retained, and tied DOF vectors, ($\underline{\mathrm{d}}$, $\underline{\mathrm{d}}_{\mathrm{R}}$, $\underline{\mathrm{d}}_{\mathrm{T}} = \underline{\mathrm{d}} \setminus \underline{\mathrm{d}}_{\mathrm{R}}$, respectively) is overloaded with both its DOF and DOF index (ordered) set counterparts, thus allowing e.g. the $d_i \in \underline{\mathrm{d}}_{\mathrm{R}}$ notation in a vector element context, and the $i \in \underline{\mathrm{d}}_{\mathrm{R}}$ notation in an integer index context.

Also an inhomogeneous Δ_j term is provided for each of the Eqns. 123 in order to accommodate constraints of the nonzero fixed displacement kind, or inhomogeneous in general.

We now define a permutation matrix $\underline{\underline{\mathrm{E}}}$ that segregates the retained and the tied $\underline{\mathrm{d}}$ elements at the head and at the tail of a reordered DOF vector, as in

$$\begin{bmatrix} \underline{\mathrm{d}}_{\mathrm{R}} \\ \underline{\mathrm{d}}_{\mathrm{T}} \end{bmatrix} = \underbrace{\begin{bmatrix} \underline{\underline{\mathrm{E}}}_{\mathrm{R}} \\ \underline{\underline{\mathrm{E}}}_{\mathrm{T}} \end{bmatrix}}_{\underline{\underline{\mathrm{E}}}} \underline{\mathrm{d}} \qquad\qquad \underline{\mathrm{d}} = \underbrace{\begin{bmatrix} \underline{\underline{\mathrm{E}}}_{\mathrm{R}}^{\top} & \underline{\underline{\mathrm{E}}}_{\mathrm{T}}^{\top} \end{bmatrix}}_{\underline{\underline{\mathrm{E}}}^{\top} \equiv \underline{\underline{\mathrm{E}}}^{-1}} \begin{bmatrix} \underline{\mathrm{d}}_{\mathrm{R}} \\ \underline{\mathrm{d}}_{\mathrm{T}} \end{bmatrix},$$

where the $\underline{\underline{\mathrm{E}}}$ block partitioning is s.t.

$$\underline{\mathrm{d}}_{\mathrm{R}} = \underline{\underline{\mathrm{E}}}_{\mathrm{R}} \underline{\mathrm{d}} \qquad\qquad \underline{\mathrm{d}}_{\mathrm{T}} = \underline{\underline{\mathrm{E}}}_{\mathrm{T}} \underline{\mathrm{d}},$$

and where the inverse relation is obtained based on the permutation matrix orthogonality.

By creating a m rows, $n - m$ columns matrix $\underline{\underline{\Lambda}}_{\mathrm{TR}}$ out of the λ_{ji} factors, and by stacking the Δ_j inhomogeneous terms into a $\underline{\Delta}_{\mathrm{R}}$ column vector, the following alternative expression is obtained for the Eqns. 123

$$\underline{\mathrm{d}}_{\mathrm{T}} = \underline{\underline{\Lambda}}_{\mathrm{TR}} \underline{\mathrm{d}}_{\mathrm{R}} + \underline{\Delta}_{\mathrm{T}} \tag{124}$$

or, by abandoning the tied/retained DOF labeling and segregation,

$$\left(\begin{bmatrix} -\underline{\underline{\Lambda}}_{\mathrm{TR}} & \underline{\underline{\mathrm{I}}} \end{bmatrix} \underline{\underline{\mathrm{E}}} \right) \underline{\mathrm{d}} = \underline{\underline{\mathcal{L}}}^{\top} \underline{\mathrm{d}} = \underline{\Delta}_{\mathrm{T}}. \tag{125}$$

In the above, the m rows, n columns $\underline{\underline{\mathcal{L}}}$ matrix is also defined which will be of employed below.

The following algebraic relation may even[51] be derived, that defines the initial, unabridged $\underline{\mathrm{d}}$ DOF vector terms based on the subset that produces the retained DOF vector $\underline{\mathrm{d}}_{\mathrm{R}}$

$$\begin{aligned} \underline{\mathrm{d}} &= \left(\underline{\underline{\mathrm{E}}}^{\top} \begin{bmatrix} \underline{\underline{\mathrm{I}}} \\ \underline{\underline{\Lambda}}_{\mathrm{TR}} \end{bmatrix} \right) \underline{\mathrm{d}}_{\mathrm{R}} + \left(\underline{\underline{\mathrm{E}}}^{\top} \begin{bmatrix} \underline{0} \\ \underline{\Delta}_{\mathrm{T}} \end{bmatrix} \right) \\ &= \underline{\underline{\Lambda}} \, \underline{\mathrm{d}}_{\mathrm{R}} + \underline{\Delta}; \end{aligned} \tag{126}$$

the $\underline{\Delta}$ n-sized column vector collects the various Δ_j terms of the 123 constraint equations, and the n rows, $n-m$ columns $\underline{\underline{\Lambda}}$ matrix collects

[51] The author is really sorry for the prolification of the defined symbols, which all carry, in slightly different forms and for slightly different purposes, the same information.

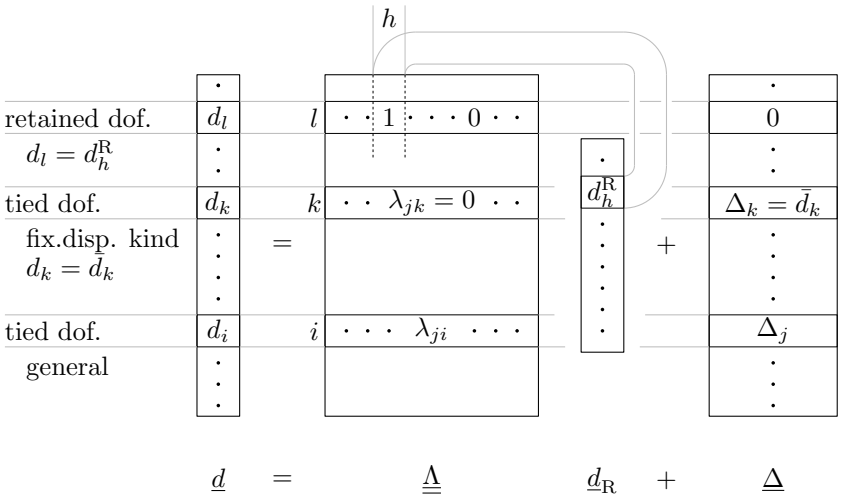

Figure 16: Graphical representation for the $\underline{\underline{\Lambda}}$ matrix in Eq. 126; representative matrix rows are illustrated for a retained DOF, and for two tied DOFs, namely a fixed displacement subcase, and the general case.

- the identity relations between corresponding retained DOFs terms that appear in both $\underline{\mathrm{d}}$ and $\underline{\mathrm{d}}_{\mathrm{R}}$, and
- the λ_{ji} coefficients that define the linear variation dependence of the tied d_j DOF on the retained d_i DOF.

Figure 16 illustrates a few representatives of the rows whose assembly defines the $\underline{\underline{\Lambda}}$. In the case of a retained global DOF, d_l, which finds a counterpart in the h-th element of $\underline{\mathrm{d}}_{\mathrm{R}}$, $= d_h^{\mathrm{R}}$, the associated row contains a single unit term at of the intersection of the l-th row with the h-th column, being zero elsewhere. In the case of a tied DOF of the plain fixed displacement kind (single DOF constraint), the associated row in $\underline{\underline{\Lambda}}$ is null, and the associated inhomogeneous term in $\underline{\Delta}$ equates the imposed value for the displacement. In the case of a tied DOF of the general kind, see Eq. 126, the associated row in the $\underline{\underline{\Lambda}}$ matrix is build upon the λ_{ji} linear relation coefficients.

It is finally worth to mention that the virtual displacements in the neighborhood of a feasible constrained configuration are restricted to

the linear combinations of the $\underline{\underline{\Lambda}}$ matrix columns $\underline{\Lambda}_j$, i.e.

$$\delta\underline{\mathrm{d}} = \underline{\underline{\Lambda}}\,\delta\underline{\mathrm{d}}_R = \underline{\Lambda}_1\,\delta d_1^R + \underline{\Lambda}_2\,\delta d_2^R + \dots \tag{127}$$

with arbitrary virtual displacement values δd_j^R for the retained DOF alone.

The ideal constraint hypothesis requires the reaction force vector $\underline{\mathrm{R}}$ to be orthogonal to a generic virtual displacement, and such condition hods if and only if $\underline{\mathrm{R}}$ is orthogonal to each the $\underline{\underline{\Lambda}}$ matrix columns, i.e.

$$\langle\,\underline{\Lambda}_j,\,\underline{\mathrm{R}}\,\rangle = 0 \quad \forall j, \tag{128}$$

or, equivalently,

$$\underline{\underline{\Lambda}}^{\top}\,\underline{\mathrm{R}} = \underline{0}\,. \tag{129}$$

Also, the homogeneous counterpart of 125 hold for the same virtual displacements, namely

$$\underline{\underline{\mathcal{L}}}^{\top}\delta\underline{\mathrm{d}} = \underline{0}\,, \tag{130}$$

to be orthogonal to the $\underline{\underline{\mathcal{L}}}$ matrix columns, but otherwise free; the linear span of those columns thus contains all and the only reaction vectors that are orthogonal (and, in particular work-orthogonal) to any feasible virtual displacement. We hence have that the variation of the m terms of a $\underline{\ell}$ column vector makes

$$\underline{\mathrm{R}} = -\underline{\underline{\mathcal{L}}}\,\underline{\ell}\,, \tag{131}$$

span all the allowed ideal constraint reaction subspace[52].

Due to their role in defining the $\underline{\underline{\mathcal{L}}}$ matrix, the λ_{ji} coefficients that drive the homogeneous part of Eqs. 123 kinematic relations also rule the allowed internal and external reaction forces. In particular, for each j-th tied DOF ($j \in \underline{\mathrm{d}}_{\mathrm{T}}$) a parametric constraint reaction $\underline{\mathrm{R}}^j$ is raised in the form

$$\begin{aligned} R_j^j &= -\ell_j \\ R_k^j &= 0 \qquad k \in \underline{\mathrm{d}}_{\mathrm{T}} \setminus \{j\} \\ R_i^j &= \lambda_{ji}\ell_j \quad i \in \underline{\mathrm{d}}_{\mathrm{R}}, \end{aligned} \tag{132}$$

to enforce the associated equation; the overall reaction force vector $\underline{\mathrm{R}}$ is obtained as the accumulation of the $\underline{\mathrm{R}}^j$ contributions. The ℓ_j factors may be obtained from the solution of the equilibrium equations.

[52] the inclusion of a minus sign does not really require a justification, due to the arbitrary nature of $\underline{\ell}$.

0.8 The system of constrained equilibrium equations, and its solution.

The nodal DOF equilibrium equations derived by pairing i) the $\underline{\underline{\mathrm{K}}}\,\underline{\mathrm{d}}$ external forces required to keep the structure in a $\underline{\mathrm{d}}$ deformed configuration, see Eq. 118, ii) the actual external forces $\underline{\mathrm{F}}$ which are applied to the elements as distributed loads, see Eq. 121, or directly at nodes in form of concentrated loads, and iii) the reaction forces $\underline{\mathrm{R}}$ may be cast as

$$\underline{\underline{\mathrm{K}}}\,\underline{\mathrm{d}} = \underline{\mathrm{F}} + \underline{\mathrm{R}}\,. \tag{133}$$

Here, $\underline{\mathrm{d}}$ and $\underline{\mathrm{R}}$ are both unknown.

If constraints are applied, we have

$$\underline{\underline{\mathrm{K}}}\,\left(\underline{\underline{\Lambda}}\,\underline{\mathrm{d}}_{\mathrm{R}} + \underline{\Delta}\right) = \underline{\mathrm{F}} + \underline{\mathrm{R}} \tag{134}$$

and

$$\underline{\underline{\mathrm{K}}}\,\underline{\underline{\Lambda}}\,\underline{\mathrm{d}}_{\mathrm{R}} = \left(\underline{\mathrm{F}} - \underline{\underline{\mathrm{K}}}\,\underline{\Delta}\right) + \underline{\mathrm{R}}\,, \tag{135}$$

where the inhomogeneous part of the constraint equations is *de facto* assimilated to a further contribution to the external loads, which may be rationalized as the elastic nodal reactions raised when i) all the retained DOF are kept fixed at their initial position, and ii) each tied DOF is displaced of an amount equal to the inhomogeneous term of the tying equation.

By projecting the equations on the subspace of allowed configurations

$$\underbrace{\underline{\underline{\Lambda}}^{\top}\,\underline{\underline{\mathrm{K}}}\,\underline{\underline{\Lambda}}}_{\underline{\underline{\mathrm{K}}}_{\mathrm{R}}}\,\underline{\mathrm{d}}_{\mathrm{R}} = \underbrace{\underline{\underline{\Lambda}}^{\top}\left(\underline{\mathrm{F}} - \underline{\underline{\mathrm{K}}}\,\underline{\Delta}\right)}_{\underline{\mathrm{F}}_{\mathrm{R}}} + \underbrace{\underline{\underline{\Lambda}}^{\top}\,\underline{\mathrm{R}}}_{=0}\,, \tag{136}$$

the contribution of the unknown reaction forces, that are normal to such a subspace – see Eq. 129, vanishes.

The linear system of *constrained* nodal DOF equilibrium equations is then set as

$$\underline{\underline{\mathrm{K}}}_{\mathrm{R}}\,\underline{\mathrm{d}}_{\mathrm{R}} = \underline{\mathrm{F}}_{\mathrm{R}} \tag{137}$$

and it may be solved for the retained DOF vector $\underline{\mathrm{d}}_{\mathrm{R}}$.

Once the solution vector $\underline{\mathrm{d}}^{*}_{\mathrm{R}}$ is found in terms of displacements at retained DOFs, the overall displacement vector and the unknown reaction forces may be derived as

$$\underline{\mathrm{d}}^{*} = \underline{\underline{\Lambda}}\,\underline{\mathrm{d}}^{*}_{\mathrm{R}} + \underline{\Delta}\,; \tag{138}$$

and

$$\underline{\mathrm{R}}^{\,*} = \underline{\underline{\mathrm{K}}}\,\left(\underline{\underline{\Lambda}}\,\underline{\mathrm{d}}_{\mathrm{R}}^{\,*} + \underline{\Delta}\right) - \underline{\mathrm{F}}\,. \tag{139}$$

0.9 An alternative constraining formulation

which reveals itself consistent with the Lagrange multiplier technique for constrained minimization.

Differences with respect to the previous one are:

- more classical and widespread in literature;
- constraint equations are treated as, indeed, equations, and not as DOF assignments; in particular the DOFs are not to be partitioned into the *tied*/*retained* sets. Such a distinction is however a fact in actual implementations;
- the order of the system of equations to be solved is augmented (vs. reduced) of one unit for each added constraint; the impact on the matrix bandwidth is however analogous;
- the assembled stiffness matrix is bordered with further minors, but not otherwise manipulated;
- the basis for the reaction force vectors clearly appears from the formulation.

The Eq. 131 form for the reaction forces is substituted within the nodal equilibrium equations 133, thus obtaining the following

$$\underline{\underline{\mathrm{K}}}\,\underline{\mathrm{d}} + \underline{\underline{\mathcal{L}}}\,\underline{\ell} = \underline{\mathrm{F}}$$

under-determined system of n equations in the $n+m$ unknowns $\underline{\mathrm{d}}$ and $\underline{\ell}$. By appending the m constraint equations 125, cardinality consistency between equation number and unknowns is restored, thus leading to the linear system of equations

$$\begin{bmatrix} \underline{\underline{\mathrm{K}}} & \underline{\underline{\mathcal{L}}} \\ \underline{\underline{\mathcal{L}}}^{\top} & \underline{\underline{0}} \end{bmatrix} \begin{bmatrix} \underline{\mathrm{d}} \\ \underline{\ell} \end{bmatrix} = \begin{bmatrix} \underline{\mathrm{F}} \\ \underline{\Delta}_{\mathrm{T}} \end{bmatrix}, \tag{140}$$

whose order is $n+m$.

The educated reader might recognise in 140 the system of equations associated to the retrieval of the stationary point in the $\underline{\mathrm{d}}$, $\underline{\ell}$ variables of the following quadratic form

$$\frac{1}{2}\,\underline{\mathrm{d}}^{\top}\,\underline{\underline{\mathrm{K}}}\,\underline{\mathrm{d}} - \underline{\mathrm{d}}^{\top}\,\underline{\mathrm{F}} + \underline{\ell}^{\top}\left(\underline{\underline{\mathcal{L}}}^{\top}\,\underline{\mathrm{d}} - \underline{\Delta}_{\mathrm{T}}\right), \tag{141}$$

which in turn represents – according to the Lagrange multiplier technique – the minimization of the total potential energy of a linearly elastic system

$$\frac{1}{2}\,\underline{\mathrm{d}}^{\top}\,\underline{\underline{\mathrm{K}}}\,\underline{\mathrm{d}} - \underline{\mathrm{d}}^{\top}\,\underline{\mathrm{F}}$$

i.e. the sum of i) internal strain energy, and ii) the unexerted work aka. the potential of the external forces, subject to the

$$\underline{\underline{\mathcal{L}}}^{\top}\,\underline{\mathrm{d}} - \underline{\Delta}_{\mathrm{T}} = \underline{0}$$

kinematic constraints, being $\underline{\ell}$ the vector obtained by stacking the Lagrange multipliers.

0.10 Retrieval of element based results

Once the problem is solved in terms of the $\underline{\mathrm{d}}^{*}$ structure nodal displacements, we may extract for each j-th element the associated local DOFs vector as

$$\underline{\mathrm{d}}^{*}_{\mathrm{e}j} = \underline{\underline{\mathrm{P}}}_{\mathrm{e}j}\,\underline{\mathrm{d}}^{*}. \tag{142}$$

We may in turn derive the strains at the reference plane, and the curvatures as

$$\underline{\mathrm{e}} = \underline{\underline{\mathrm{B}}}^{e}_{\mathrm{e}j}(\xi,\eta)\,\underline{\mathrm{d}}^{*}_{\mathrm{e}j} \qquad\qquad \underline{\kappa} = \underline{\underline{\mathrm{B}}}^{\kappa}_{\mathrm{e}j}(\xi,\eta)\,\underline{\mathrm{d}}^{*}_{\mathrm{e}j} \tag{143}$$

or directly the TT, IP strain components as

$$\underline{\epsilon} = \left(\underline{\underline{\mathrm{B}}}^{e}_{\mathrm{e}j}(\xi,\eta) + \underline{\underline{\mathrm{B}}}^{\kappa}_{\mathrm{e}j}(\xi,\eta)z\right)\,\underline{\mathrm{d}}^{*}_{\mathrm{e}j}. \tag{144}$$

IP stresses may be then derived according to the material constitutive law, see Eq. 13. The OOP tranverse shear strain components may be derived as

$$\underline{\gamma}_{z} = \underline{\underline{\mathrm{B}}}^{\gamma}_{\mathrm{e}j}(\xi,\eta)\,\underline{\mathrm{d}}^{*}_{\mathrm{e}j}. \tag{145}$$

All the cited quantities are customarily sampled at the gaussian integration points, and possibly extrapolated at nodes.

0.11 Notable Multi Point Constraints

0.11.1 Rigid body link RBE2

A master (or retained, control, independent, etc.) C node is considered, whose coordinates are defined as x_C, y_C, z_C in a (typically) global reference system, along with a set of n P_i nodes whose coordinates are x_i, y_i, z_i.

A kinematic link is to be established such that the DOFs – or a subset of them – associated to the P_i nodes follow the rototranslations of the C control according to the rigid body motion laws.

In the case of a fully constrained P_i node we have

$$\begin{bmatrix} u_i \\ v_i \\ w_i \\ \theta_i \\ \phi_i \\ \psi_i \end{bmatrix} = \underbrace{\begin{bmatrix} 1 & 0 & 0 & 0 & +(z_i - z_C) & -(y_i - y_C) \\ 0 & 1 & 0 & -(z_i - z_C) & 0 & +(x_i - x_C) \\ 0 & 0 & 1 & +(y_i - y_C) & -(x_i - x_C) & 0 \\ 0 & 0 & 0 & 1 & 0 & 0 \\ 0 & 0 & 0 & 0 & 1 & 0 \\ 0 & 0 & 0 & 0 & 0 & 1 \end{bmatrix}}_{\underline{\underline{\mathrm{L}}}_i} \cdot \begin{bmatrix} u_C \\ v_C \\ w_C \\ \theta_C \\ \phi_C \\ \psi_C \end{bmatrix} \tag{146}$$

where u, v, w (θ, ϕ, ψ) are the translation (rotation) vector components with respect to the x, y, z cartesian reference system. A subset of the above DOF dependency relations may be cast to obtain a partial constraining of the P_i node; a free relative motion of such node with respect to the rigid body is allowed at the unconstrained DOFs.

External actions that are applied to tied P_i DOFs are reduced to the master node in form of a statically equivalent counterpart; the contributions deriving from each P_i node are finally accumulated.

0.11.2 Distributed load / averaged motion link RBE3

A *reference* C node, whose coordinates are x_C, y_C, z_C. A distribution of n *weighted* nodes P_i, q_i is considered, whose coordinates are x_i, y_i, z_i. The nodal weight q_i is usually determined with some degree of arbitrariness, e.g. based on partitioning the attached elements into nodal influence domains, and associating to each node a weight which is proportional to pertaining volumes, areas or edge lengths.

The RBE3 multi-DOF constraint may be described based on i) the imposed kinematic relations and ii) on the nature of the associated reaction force.

Starting from the latter, a generic load applied at C, namely three force components U_C, V_C, W_C and three moment components Ω_C, Φ_C, Ψ_C. A suitable set of reaction forces is induced that balance at C the applied actions, and distributes them at the P_i nodes based on the relation

$$\begin{bmatrix} U_i \\ V_i \\ W_i \end{bmatrix} = q_i \left(\begin{bmatrix} a \\ b \\ c \end{bmatrix} + \begin{bmatrix} 0 & d & -f \\ -d & 0 & e \\ f & -e & 0 \end{bmatrix} \begin{bmatrix} x_i \\ y_i \\ z_i \end{bmatrix} \right), \tag{147}$$

with a, b, c, d, e, f coefficients that are defined based on the static equivalence of the applied load at C, and its distributed counterpart; in particular the system of six linear equations

$$\begin{bmatrix} U_C \\ V_C \\ W_C \end{bmatrix} = \sum_i \begin{bmatrix} U_i \\ V_i \\ W_i \end{bmatrix}, \qquad \begin{bmatrix} \Theta_C \\ \Phi_C \\ \Psi_C \end{bmatrix} = \sum_i \begin{bmatrix} U_i \\ V_i \\ W_i \end{bmatrix} \wedge \begin{bmatrix} x_i - x_C \\ y_i - y_C \\ z_i - z_C \end{bmatrix} \tag{148}$$

is solved for the aforementioned unknown parameters.

In the case a reference system is employed whose x, y, z axis are principal of inertia with respect to the same distribution, a more substantial description may be provided as follows... TODO.

Bibliography

[1] S. Timoshenko, S. Timoshenko, and J. Goodier, *Theory of Elasticity, by S. Timoshenko and JN Goodier,...* McGraw-Hill book Company, 1951.

[2] S. Vlachoutsis, "Shear correction factors for plates and shells," *International Journal for Numerical Methods in Engineering*, vol. 33, no. 7, pp. 1537–1552, 1992.

[3] T. Chow, "On the propagation of flexural waves in an orthotropic laminated plate and its response to an impulsive load," *Journal of Composite Materials*, vol. 5, no. 3, pp. 306–319, 1971.

[4] V. Birman and C. W. Bert, "On the choice of shear correction factor in sandwich structures," *Journal of Sandwich Structures & Materials*, vol. 4, no. 1, pp. 83–95, 2002.

[5] C. Hua, "An inverse transformation for quadrilateral isoparametric elements: analysis and application," *Finite elements in analysis and design*, vol. 7, no. 2, pp. 159–166, 1990.

[6] B. M. Irons and A. Razzaque, "Experience with the patch test for convergence of finite elements," in *The mathematical foundations of the finite element method with applications to partial differential equations*, pp. 557–587, Elsevier, 1972.

[7] C. Militello and C. A. Felippa, "The individual element test revisited," in *The finite element method in the 1990's*, pp. 554–564, Springer, 1991.

[8] R. MacNeal, *Finite Elements*. CRC Press, 1993.

[9] T. J. Hughes and T. Tezduyar, "Finite elements based upon mindlin plate theory with particular reference to the four-node bilinear isoparametric element," *Journal of applied mechanics*, vol. 48, no. 3, pp. 587–596, 1981.